Published in final edited form as:
J Immunol. 2013 July 1; 191(1): 434–447. doi:10.4049/jimmunol.1203176.

Optimal Germinal Center B cell Activation and T-dependent Antibody Responses Require the Expression of the Mouse Complement Receptor Cr1*

Luke R. Donius, **Jennifer M. Handy**, **Janis J. Weis**, and **John H. Weis**
The Division of Cell Biology and Immunology, Department of Pathology, University of Utah School of Medicine, Salt Lake City, UT 84112

Abstract

Follicular dendritic cells and complement receptors 1 and 2 are important for the generation of humoral immunity. Cr1/2 expression on B cells and FDC has been shown to provide a secondary signal for B cell activation, to facilitate transport of antigen in immune follicles, and to enhance retention of immune complexes by FDC. We show here that murine B cells predominantly express the Cr2 product from the *Cr2* gene while FDC nearly exclusively express the Cr1 isoform generated from the *Cr2* gene. To define the specific role of Cr1, we have created an animal that maintains normal cell restricted expression of Cr2 but does not express Cr1. Cr1 deficient (*Cr1KO*) mice develop normal B1 and B2 immature and mature B cell subsets, and have normal levels of naïve serum antibodies but altered levels of natural antibodies. Immunization of the *Cr1KO* animal demonstrates deficient antibody responses to T-dependent but not T-independent antigens. Germinal centers from the immunized *Cr1KO* animal possess a deficiency in activated B cells, similar to that seen for the animal lacking both Cr1 and Cr2, or C3. Finally, animals lacking only Cr1 respond similar to the WT animal to infections with *Streptococcus pneumoniae*, a pathogen that animals lacking C3 or both Cr1 and Cr2 are particularly sensitive to. These data, in total, suggest that the production of Cr1 primarily by FDC is critical in the generation of appropriately activated B cells of the germinal center and the generation of mature antibody responses.

Introduction

Antibodies (immunoglobulins) are the major effectors of the adaptive immune response and the production of different isotype classes of antibody are produced in order to achieve different effects with antibody of the same specificity. Immunoglobulin class-switch recombination (CSR) is a hallmark of B cell responses to T-dependent antigens (1). These reactions occur within immune follicles of secondary immune structures such as the spleen and lymph nodes (2). Central to follicles are follicular dendritic cells (FDC) which establish the zonal identity (3) and act as a concentrated depot of antigen. In the course of an immune challenge antigen is trafficked to the FDCs (4–6), where follicular B cells are recruited for surveillance of retained antigen. B cell receptor (BCR) specificity for an antigen retained on an FDC results in internalization and processing for presentation to T cells. The B cell then

*This work was supported by Public Health Service Grants AI-24158 and AI-088451 (to J.H.W.), AI-32223 and AI-43521 (to J.J.W.), the Training Program in Microbial Pathogenesis 5T32-AI-055434 (L.R.D.) and funds from the George J. Weber Presidential Endowed Chair (J.H.W.).

Address correspondence:john.weis@path.utah.edu.

Disclosures
The authors have no financial conflicts of interest.

migrates to the T cell zone and presents the processed peptide to helper T cells in the context of class II MHC. Upon a secondary signal from a peptide specific helper T cell this B cell will undergo somatic hypermutation and isotype switch. These activated germinal center (GC) B cells must then re-test their new immunoglobulin before undergoing clonal expansion and differentiation to either a plasma or memory cell. FDCs play an integral role in retention of antigen for this 'test' of the new immunoglobulin as well. Transport to and capture of antigen by FDCs in a primary immune response utilizes the protein products of the mouse *Cr2* gene, complement receptor 1 (Cr1) and Cr2 (4).

The predominant role of the complement cascade is detection of danger signals via the classical, mannose-binding lectin, and alternative pathways and targeting of bound cells for lytic killing by the membrane attack complex (MAC) (7–9). However, in addition to targeting foreign cells for MAC lysis, opsonization by the protein complement component 3 (C3) can be utilized in transport to an FDC, phagocytosis, secondary signals through various complement receptors, and activation of more complement. These outcomes are dependent on the cleavage fragment of C3 and the corresponding cell receptor they encounter. C3 is central to all three complement pathways and upon activation it is cleaved into C3b and C3a. C3a is a potent anaphylatoxin that diffuses away to recruit and activate cells, while C3b remains bound to the foreign molecule and forms a C3 convertase complex that cleaves more C3. Alternatively, in the presence of the complement regulator, factor I (Cfi), and one of the co-factors - factor H, Crry, or Cr1 - C3b can be further cleaved into one of the enzymatically inactive fragments: iC3b or C3d(g). Activation of the complement pathway can modulate humoral immunity (10) through the complement receptors 1 and 2 (Cr1 and Cr2) (11–14). Both Cr1 and Cr2 can bind the terminal cleavage products of C3, iC3b, and C3d(g). In addition Cr1 is capable of binding the enzymatically active C3 convertase subunit C3b and acting as a cofactor for factor I cleavage of C3b to iC3b or C3d(g) (15).

The mouse differs from the human in that the single mouse *Cr2* gene encodes both Cr1 and Cr2 via alternative splicing while primates utilize distinct genes for the CR1 and CR2 proteins (16). Expression of the mouse *Cr2* gene by B cells and FDC has long been held under the assumption that the two different isoforms, Cr1 and Cr2, are produced equally in both of these distinct cell types. Functionally, mouse knockout models have addressed the loss of both Cr1 and Cr2 when critical sequences of the *Cr2* gene have been deleted (12, 13). These studies have not delineated the specific functions of the Cr1 and Cr2 proteins on B cells and FDC, and elevated surface expression of CD19 on *Cr1/2KO* B cells has been proposed to lead to B cell anergy (17). Additional studies have also utilized Cr1/2 deficient (*Cr1/2KO*) animals to examine the function of human CR1 or CR2 via transgenic expression models of these proteins using immunoglobulin gene promoters (18, 19). In these studies, however, premature expression of the transgenes (compared to native *Cr2*), lack of FDC expression, expression in inappropriate cell types (T cells, etc), and the structural distinctness of human CR1 compared to the mouse Cr1 protein introduces critical variables. In light of these variables neither of the human CR1 or CR2 transgenic models elucidate the individual functions of the Cr1 and Cr2 proteins (mouse or human) in the context of their autochthonous immune response.

To directly assess the phenotype of an animal lacking Cr1, but expressing Cr2 under the endogenous transcriptional controls of the *Cr2* gene, we have created a novel mouse Cr1 knockout model (*Cr1KO*) in which the exons encoding the domains unique to the Cr1 protein have been removed forcing *Cr2* gene transcripts to splice from the exon encoding the signal sequence to the exon encoding the first domain of the Cr2 protein. The validation of the *Cr1KO* animal showed a complete lack of that protein in such mice. Comparison of this animal to WT demonstrated the Cr1 protein on FDC and Cr2 protein on B cells as the dominant *Cr2* gene isoforms on these cell types in the native animal. *Cr1KO* mice display

numerous phenotypes that are different from the WT and *Cr1/2KO* mice. *Cr1KO* mice do not exhibit the antibody response deficiencies to T-independent and low dose T-dependent antigens that are hallmarks of *Cr1/2KO* mice. *Cr1KO* mice also do not produce WT levels of antibody against a high dose of T-dependent antigen, and generate fewer activated B cells in response to T-dependent antigens. Additionally the *Cr1KO* mice do not suffer from the reduced immunity to the bacterial pathogen *Streptococcus pneumoniae* as *Cr1/2KO* mice do. In total these studies describe a new mouse strain specifically deficient in Cr1 but not Cr2, demonstrate a novel Cr1 expression preference by FDC compared to Cr2 and further support that Cr1 is an important surface protein required for the generation of an optimal humoral immune response.

Materials and Methods

Generation of Cr1KO Mice

A 21kB construct was built in the pBluescriptII KS+ vector. Homologous recombination was targeted to the intronic EcoRV restriction fragment of the *Cr2* gene 5' to exon 2 and the NheI restriction fragment 3' to exon 8 in order to delete exons 2 through 8 while leaving the sequence for splicing of *Cr2* (Fig. 1A). These fragments were fused to the germline self-deleting neomycin containing pACN positive selection vector (20). Targeted homologous recombination was enhanced by the flanking TK1TK2 thymidine kinase expressing negative selection vector. The pACN and TK1TK2 vectors were obtained from the University of Utah Transgenic and Gene Targeting Mouse Core. The linearized construct was targeted to mouse strain 129 derived embryonic stem cells by electroporation and 192 clones were screened by Southern Blot for homologous recombination of the *Cr1KO* construct. Chimeras were generated via injection of a positive clone into blastocyst and surrogate implantation. Electroporation, blastocyst injection, and chimera generation was performed by the University of Utah Transgenic and Gene Targeting Mouse Core. The *Cr1KO* construct insertion was tracked via PCR of DNA isolated from tail biopsies. Primers flanking exon 2, upstream of the EcoRV site (#4150 5'-TAGTGTGAGACGGAATCTTAACAC-3') and exon 8, downstream of the NheI site #4316 5'-GCAGGTAGCACAGTTACATTAGATAC-3') were designed to amplify a 483bp fragment upon recombination for identification of the *Cr1KO* condition. The WT allele was identified with a primer from coding sequences in exon 8 (#4404 5'-TGGAATAATAAGTTTCCTGTCTGTG-3') and a primer in the adjacent intron between exons 8 and 9 but upstream of the NheI site (#4422 5'-AGAACTCTTCAGTAAAAGGCATGAC-3') that generated a 350bp product. All experiments were carried out using *Cr1KO* mice backcrossed to C57BL/6 or BALB/C for at least 5 generations. Wildtype C57BL/6 and BALB/C as well as complement component 3 deficient (*C3KO*) mice were purchased from The Jackson Laboratory (Bar Harbor, ME) or obtained from colonies bred on location. All mice used in experiments were C57BL/6 derived (*Cr1KO, Cr1/2KO, C3KO* and WT)(12) 8 to 16 week old male and female mice unless otherwise specified. Mice were sex matched across genotypes. All mice were housed at the Comparative Medicine Center (University of Utah Health Sciences Center) in accordance with the National Institutes of Health guidelines for the care and use of laboratory animals. Mice were housed in an Animal Biosafety Level 2 protocol approved area for all *Streptococcus pneumoniae* infection experiments.

Total Splenic Protein Isolation

Splenic protein isolation, with FDC included, was performed by extracting approximately two thirds of a spleen (RNA was isolated from the remaining third using the method described above) from a mouse and disrupting it with a razor blade in 5ml of ice cold PBS. The dissociated spleen was then pipetted into a 15ml conical, centrifuged at 300g, and the

supernatant was discarded. The dissociated spleen was resuspended in 300μl of RIPA buffer containing protease inhibitors (complete, mini, EDTA-free, ultra tablets; Roche Diagonostics, Indianapolis IN), transferred to a 1.5ml microcentrifuge tube, and placed in a rotator at 4°C for 45 minutes. The solubilized protein was then isolated by centrifugation of the lysate at high speed and 4°C in a microcentrifuge for 10 minutes and collecting the supernatant. The resulting protein isolate was stored at −70°C until Western blot analysis.

Bone Marrow Transplantation

Transplant recipients were lethally irradiated 24 hours prior to transplantation with two doses of 500 cGy with an X-ray irradiator. Bone marrow donor mice were sacrificed and marrow was isolated from the femurs and tibias. Red blood cells were lysed with ACK lysis buffer, the remaining cells were washed, strained through 100μm mesh, and resuspended in about 300μl of PBS per mouse. Each recipient mouse was anesthetized with isofluorane and given 100μl of sex matched bone marrow retro-orbitally. One donor was transplanted into up to three recipients. Mice were maintained on antibiotic water and engraftment was allowed for six weeks.

Quantitative RT-PCR

Total spleen RNA was isolated using the CsCl centrifugation method as described previously (21). Briefly, spleens were isolated from mice and homogenized using a tissuemizer in 4M guanidine isothiocyanate solution and centrifuged at 30,000RPM overnight on a 5.7M CsCl gradient. The RNA pellet was recovered, resuspended in 400μl nuclease free water with 0.2M NaCl, and ethanol precipitated for 3 hours. The RNA was pelleted at high speed in a microcentrifuge, washed with 70% ethanol, and resuspended in 50μl of nuclease free water. cDNA was generated as previously described (22). Quantification of transcript levels for *Cr1, Cr2, Cr1/2, Alox5, Dbp, Ctsg, Fv, Lcn2, Klra18*, and *β-actin* was measured using a Roche Lightcycler (Indianapolis, IN) as previously described (21, 23). Primers for PCR of total *Cr1/2* transcript were #4824 5'-AAGGAAGCAAAACTGTCTGGTGC-3' and #4825 5'-CCCGCAACAAACTGGTCAAC-3'. Primers for PCR of *Cr1* and *Cr2* specific transcripts were as previously published (22, 24, 25). PCR primers for quantification of *Alox5, Dbp, Ctsg, Fv, Lcn2, Klra18*, and *β-actin* were as previously published (25).

Western Blot Analysis

Western Blot analysis was performed as previously described (22). For Cr1/2 protein detection the membrane was blocked in 5% milk 0.2% Tween-20 in 1X Tris-buffered saline (TBS). Cr1/2 were detected with goat polyclonal anti-CD21 (Santa Cruz Biotechnology #sc-7027) and visualized with the horseradish peroxidase conjugated secondary antibody bovine anti-goat IgG (Jackson ImmunoResearch #805-035-180).

Immunohistochemistry

Spleens were prepared by fixing in 4% paraformaldehyde and dehydrating in 5%, 15%, and 30% sucrose in PBS. Spleens were then frozen on dry ice in OCT embedding medium (Sakura Finetek USA, Inc. Torrance CA) and stored −70°C. Frozen spleens were sectioned on a cryostat at a width of 10–12μm. Spleen sections were rehydrated in 0.1% Tween-20 in 1X PBS (PBT). Treated with H_2O_2 in PBT, washed three times with PBT, and blocked with 1% BSA 1:50 anti-CD16/32 (Fc Block; eBioscience clone #93) for 1 hour. Blocking buffer was discarded and the sections were incubated overnight with biotinylated primary antibody at 4°C (anti-Cr1/2 clone 7E9 or anti-Cr1 clone 8C12). Sections were rinsed once with PBT and then washed three times with PBT. Sections were then incubated with a 1:1000 dilution of streptavidin conjugated to horseradish peroxidase in 1% BSA PBT for 1 hour at room

temperature. Sections were washed with PBT, stained with 3, 3'-diaminobenzidine (DAB) (Vector Laboratories Burlingame, CA) as per company protocol, and counter stained with hematoxylin QS (Vector Laboratories Burlingame, CA). Sections were then overlaid with VectaMount AQ (Vector Laboratories Burlingame, CA) preservation reagent, cover-slipped, and sealed with fingernail polish.

Enzyme-linked Immunoasorbent Assays (ELISA)

ELISAs to determine total serum antibody titers and antigen specific antibody titers were performed using the same basic blocking, washing, and detection protocol. ELISA plates were prepared as follows for antigen specific antibody quantification: 5μg/ml of TNP-BSA (TNP-LPS and TNP-KLH antibody response measurement), 5μg/ml DNP-BSA (DNP-AECM-Ficoll antibody response measurement), 5μg/ml PC-BSA (Phosphorylcholine natural antibody quantification) (all conjugates from BioSearch Technologies), or 5μg/ml Keyhole Limpet Hemocyanin (Sigma-Aldrich) in 1X PBS was prepared and dispensed in volumes of 100μl per well onto Immulon 4 HBX (Thermo Scientific) plates. Sandwich ELISA plates for total serum antibody quantification were prepared by incubating plates with 5μg/ml anti-mouse IgM-IgG-IgA antibody (Pierce #31171) in carbonate buffer (15 mM Na_2CO_3 35 mM $NaHCO_3$ 3.1mM NaN_3). Polysorp plates (Thermo Scientific) for detection of chitin/chitosan specific antibody were prepared as described (26). Maxisorp plates (Thermo Scientific) for dsDNA specific antibody were coated overnight with 10μg/ml of calf thymus DNA in 1X PBS at 4°C. Plates were covered and incubated overnight at 4°C. Solution was discarded and all wells were blocked with 200μl of 5%BSA 0.1% Tween-20 in 1X PBS blocking buffer for 1 hour at room temperature. Blocking buffer was discarded and wells were washed three times with 0.1% Tween-20 in 1X PBS (ELISA wash buffer). Serum samples were then applied serially to wells in 5%BSA in 1X PBS as follows: natural antibody detection 1:50, 1:100, 1:200, and 1:400; total serum immunoglobulin IgM - 1:4000, 1:8000, 1:16000, 1:32000 and IgG subclasses - 1:2000, 1:4000, 1:8000, and 1:16000; and antigen specific immunoglobulin 1:200, 1:400, 1:800, and 1:1600. Serum was incubated in wells at room temperature for 1.5 hours. Serum was discarded and all wells were washed three times with ELISA wash buffer. Secondary antibody was diluted 1:2000 in 5%BSA in 1X PBS and 100μl was distributed to each well and incubated for 1.5 hours at room temperature. All secondary antibodies were conjugated to horseradish peroxidase: rabbit anti-mouse IgM (Jackson ImmunoResearch #315-035-049), rabbit anti-mouse IgG1 (Zymed #61-0120), rabbit anti-mouse IgG2b (Zymed #61-0320), goat anti-mouse IgG2c (Jackson ImmunoResearch #115-035-208), and goat anti-mouse IgG3 (AbD Serotec #STAR6P). The secondary solution was then discarded and the wells were washed 6 times with ELISA wash buffer. Bound secondary was then detected by exposing to 100μl of o-phenylenediamine solution (8mg o-phenylenediamine and 6.6μl H_2O_2 in 20ml of citrate buffer), stopped with 100μl of 1N HCl, and the absorbance was read at 490nm with a Biotek plate reader. The absorbance values shown were calculated by subtracting the absorbance reading at 490nm of a well without serum treatment. Positive control antibodies were: mouse IgM (eBioscience clone#11E10), purified mouse myeloma IgG1 (Invitrogen #026100), mouse IgG2b (eBioscience clone#eBMG2b), mouse IgG2c (Southern Biotech #0122-01), and mouse IgG3 (eBioscience #14-4742-85).

ELISA detection of SRBC specific antibody was done using a variation of methods described above and elsewhere (27, 28). Immulon 4HBX plates were pre-coated overnight at 4°C with 5×10^7 SRBC/100μl PBS/well. Following the overnight incubation the SRBC were fixed to the plate by adding 20μl of 1.8% glutaraldehyde to each well (taking care not to disturb the SRBC layer); bringing the final concentration of glutaraldehyde to 0.3%. After a 30 minute incubation with glutaraldehyde at room temperature the contents of each plate were discarded, and the wells were washed four times with 100μl of PBS. Wells were

blocked with 200μl of 1% BSA in PBS for one hour at room temperature. Blocking buffer was discarded and serum samples were distributed to plates in 0.05% tween 1%BSA PBS. All serum samples were diluted serially (1:50 to 1:400 for IgM and 1:200 to 1:1600 for IgG) and tested in duplicate. Non-specific IgM or IgG samples were included as negative controls. Serum samples were incubated for 2 hours at room temperature. Wells were then washed three times with PBS and 100μl 1:2000 rabbit anti-mouse IgM, Fc μ chain specific, conjugated to horseradish peroxidase (Jackson Immunoresearch #315-035-049) or 1:2000 sheep anti-mouse IgG, Fc γ chain specific, conjugated to horseradish peroxidase (Jackson Immunoresearch #515-035-071) in 0.05% tween 1% BSA PBS. After a 1.5 hour incubation at room temperature the plates were washed three times with PBS, and incubation with o-phenylenediamine solution for visualization was used as above.

Fluorescent Activated Cell Sorting (FACS

Bone marrow, peritoneal cells, or splenocytes were isolated from isofluorane anesthetized and cervically dislocated mice. Bone marrow was obtained by dissecting the femurs and tibias of mice, slicing the ends of the bones off with a razor blade, and flushing the cells from the bone with 5% bovine serum albumin (BSA; Sigma-Aldrich A7906) in phosphate buffered saline (PBS) using a 23 gauge needle. Peritoneal cells were obtained by injecting 5ml of 5%BSA PBS into the peritoneal cavity, massaging the mouse's abdomen, and retrieving the fluid from the peritoneal cavity as described in detail by Ray and Dittel (29). Splenocytes were obtained by dissecting the spleen and mashing it through a 100μm cell strainer. The red blood cells were lysed with ACK buffer (0.15M NH_4Cl 1mM $KHCO_3$ 0.1mM Na_2EDTA). Cells were washed with 5%BSA PBS and 2×10^6 cells were stained in 100μl volume of antibody or streptavidin conjugated fluorophore staining mix. Incubations were 20 minutes on ice and followed by a 5%BSA PBS wash and resuspension in 500μl 5%BSA PBS, or secondary incubation. Antibodies used for FACS were as follows: anti-CD19 (clone 1D9, eBioscience), B220 (clone RA3-6B2, BioLegend), anti-CD21/35 (clones 7G6, BD Pharmingen; 7E9, BioLegend; eBio8D9, eBioscience), anti-CD35 (clone 8C12, BD Pharmingen), anti-CD11b (clone M1/70, BioLegend and eBioscience), anti-CD5 (clone 53-7.3, eBioscience), anti-CD23 (clone B3B4, BioLegend and eBioscience), anti-IgM (clone eB121-15F9, eBioscience), anti-CD24 (clone M1/69, BioLegend and eBioscience), anti-IgD (clone 11-26c.2a, BioLegend), anti-GL7 (clone GL7, eBioscience), anti-CD16/32 (Fc receptor block, clone 93, eBioscience), and rat IgM-AlexaFluor 488 isotype control (eBRM, eBioscience). Cells were strained through 100μm mesh to disrupt cell clumps, vortexed gently with 1.5μl of 1mM DAPI for live/dead discrimination, and analyzed using a FACSCantoII (BD Biosciences). FACS data was quantified using FlowJo version 8.8.7 (Tree Star, Inc).

Streptococcus pneumoniae Culture and Preparation

S. pneumoniae were generously provided by Kristina Pierce at the University of Utah Medical Technology Laboratory. *S. pneumoniae* was presumptively reconfirmed via exhibition of alpha-hemolysis and optochin sensitivity (Taxo p-discs, BD Biosciences). The isolate was determined to be serotype 3 by the Statens Serum Institute (Copenhagen, Denmark). *S. pneumoniae* was passaged once through mice by isolating viable *S. pneumoniae* from the spleen of a lethally infected C57BL/6 mouse. Isolation was performed by straining the spleen through a 100μm strainer into sterile 5%BSA PBS, and growing serial dilutions on 5% Sheep Blood Columbia Agar plates (BD Biosciences) in a candle jar (~5% CO_2) at 37°C. 5ml of 0.5% yeast supplemented Todd-Hewitt Broth (BD Biosciences) was inoculated with one colony *S. pneumoniae* and incubated for 3 hours at 37°C in candle jar. 750μl of inoculum was transferred to 70ml of yeast supplemented Todd-Hewitt Broth and incubated 5.5 hours (adapted from (30)). 25ml of culture was diluted to 10% glycerol and frozen in 1ml aliquots in cryovials at −70°C. An additional 30ml was heat-killed at 60°C

for 2 hours, aliquotted in 1ml volumes, and frozen at −70°C. Serial dilutions were plated on 5% Blood Columbia Agar plates for quantification and heat-killed *S. pneumoniae* were plated to confirm inactivation.

Immunizations and S. pneumoniae Infections

All immunizations and infections were given intraperitoneally to two to three month old mice. Doses for T-independent and T-dependent antigen specific immunoglobulin response curves were 50μg TNP-LPS (Biosearch Technologies Novato, CA), 25μg DNP-AECM-Ficoll (Biosearch Technologies Novato, CA), 10μg TNP-KLH (Biosearch Technologies Novato, CA), and 100μg TNP-KLH (Biosearch Technologies Novato, CA). Serum for immunoglobulin titering was obtained by collecting tail vein blood into heparinized capillary tubes, centrifuging at 13,000 RPM in a microcentrifuge for 6 minutes, and collecting the supernatant. Serum was collected every seven days for 21 days. The low and high dose (10μg and 100μg) T-dependent immunizations were followed 21 days after the primary immunization with a secondary boost of the same quantity, and an additional 28 day serum collection was done to measure the secondary immunoglobulin response.

For germinal center B cell activation experiments mice were injected with 2×10^8 sheep red blood cells (Innovative Research Novi, MI). Seven days later the mice were sacrificed and splenocytes were analyzed via FACS.

Mice in *S. pneumoniae* experiments were injected with 1×10^5 heat killed *S. pneumoniae* followed ten days later by infection with 1000 CFU of *S. pneumoniae*. Mice were then monitored daily for survival.

Results

Creation and characterization of a Cr1-deficient mouse

The functions of Cr1/2 have been well established to be important in humoral immunity. To investigate the independent roles of Cr1 and Cr2 in a cell and stage specific manner for the generation of functional antibody responses, we generated a Cr1 deficient, but Cr2 sufficient, *Cr1KO* mouse line. To delete *Cr1*-specific transcripts from *Cr2* without disrupting the *Cr2* locus, a construct was produced in which DNA from the Cr2 gene promoter, transcription start site and the first coding exon (encoding the signal sequence) was fused to the germline sequences possessing the C-terminal exons specific for the Cr2 protein (Fig. 1A). Care was taken to include flanking intronic DNA so as not to disrupt sequences required for the appropriate splicing of *Cr2* transcripts. The region between these two genomic sequences (occupied by Cr1 encoding exons in the native gene) was replaced with a neomycin selection cassette that would self-delete in the sperm of targeted animals leaving behind a single Lox site. Analysis of *Cr1* and *Cr2* splenocyte transcripts in the *Cr1KO* animal was performed by quantitative RT-PCR using oligonucleotide sets specific for the *Cr1* encoding transcript, a second set specific for the *Cr2* product and a third set that includes sequences common to both *Cr1* and *Cr2* products. As expected, the *Cr1KO* animal lacked Cr1-specific transcripts and expressed higher levels of Cr2-encoding transcripts than WT (data not shown).

The absence of the Cr1 protein in the *Cr1KO* animal was verified by immunoblot analysis of total splenocytes and $B220^+$ splenocytes (Fig. 1B) using a polyclonal antibody with specificity for Cr1 and Cr2. The WT samples showed a pattern of higher quantities of Cr2 than Cr1, while the *Cr1KO* animal only exhibited expression of the Cr2 protein. FACS analysis of the expression of the Cr1 and Cr2 proteins on splenic $B220^+$ B cells was done using the Cr1-specific antibody 8C12 and the 7G6 antibody that recognizes both the Cr1 and Cr2 proteins (Fig 1C). These data demonstrate the absence of the Cr1 protein (8C12) and the

elevated surface expression of the Cr2 protein (7G6) on the *Cr1KO* cells compared with WT cells. Similar data were obtained using the anti-Cr1/Cr2 antibodies eBio8D9 and 7E9 (data not shown) indicating that Cr1 deletion results in a filling of the Cr1/2 niche with Cr2. It should be noted that the preparation of isolated splenocytes for analysis in Fig.1B,C was accomplished by straining mechanically disrupted spleens through 100 micron cell strainers prior to analysis which results in the loss of FDC from these cell populations.

Phenotypic analysis of the Cr1KO mouse

The mouse Cr1 and Cr2 proteins form complexes with CD19 on the surface of mouse B cells. The absence of Cr2 gene products on the surface of *Cr1/2KO* B cells has been linked to the elevated expression of CD19 which is proposed as one mechanism leading to reduced B cell responses to antigen (17). To determine if Cr2 sufficiency returned CD19 expression on B cells to normal in *Cr1KO* mice, we measured the mean fluorescent intensity (MFI) of CD19 staining on live $B220^+$ cells from the spleen (Supplemental Fig. 1B). The MFI of CD19 staining on the *Cr1KO* cells was somewhat less than that of WT and substantially less than that seen on the surface of the *Cr1/2KO* B cells.

Analysis of B cell subsets of the *Cr1KO* mice identified no significant differences compared to WT mice. B cells in the marrow of adult mice were examined (Fig. 2) based upon the differential expression of B220, CD43, and IgM (Fig. 2A) to delineate pro-B, pre-B, immature and mature B cells. The frequencies of each of these B cell subsets in *Cr1KO* and *Cr1/2KO* mice were not altered compared to WT mice based on ANOVA (Fig. 2B). The expression level of CD19 was also quantified on these B cell subsets (Supplemental Fig. 1A) and was shown to be identical for the four subsets of B cells except for the mature B cells which displayed a significant ($p<0.01$) reduction in expression of surface CD19 in *Cr1KO* mice and significantly ($p<0.01$) elevated expression in *Cr1/2KO* mice.

FACS analysis of the $B220^+$ $CD11b^+$ and $CD5^+$ (B1a) and $CD5^-$ (B1b) cells of the peritoneal cavity were not found at different frequencies in *Cr1KO* mice compared to WT (Fig. 3A,B). Interestingly, a significant ($p<0.001$) reduction in the frequency of B1a cells in *Cr1/2KO* mice was observed (Fig. 3B). This depression in B1a B cells had not previously been documented in the *Cr1/2KO* animals (12, 13) but has been described for the hypomorphic Cr1/2 deletion animal (31, 32). A depression in B1a cells in the *Cr1KO* animal was not observed. Quantification of the MFI of CD19 on the surface of the B1a and B1b cells from the *Cr1KO* animal did not show any significant difference compared to WT or the *Cr1/2KO* animals (Supplemental Fig. 1B).

The enumeration of mature B cell subsets of the spleen in the *Cr1KO* animal was also analyzed based upon differential staining of B220, CD23, CD24 and CD21/35 (Cr1/2) (Fig. 4). Comparable transition 1 (T1), T2, follicular mature (FOB) and marginal zone (MZB) B cell subset frequencies were found in the spleens of *Cr1KO* mice as in WT and *WT/Cr1KO* heterozygote animals (ANOVA). The expression of Cr2 in the *Cr1KO* animal was consistent with the generation of the T2 B cells at the same point in B cell maturation as WT B cells. Therefore, the loss of Cr1 on the surface of murine B cells did not alter their development or their localization within the splenic B cell populations.

We have previously shown that the spleens of *Cr1/2KO* animals displayed signatures of a more highly inflamed environment than WT, presumably due to lack of control of complement convertases in immune complexes within immune follicles (25). The analysis of total splenic transcripts for inflammatory response genes also demonstrated altered expression of inflammatory mediator genes in the *Cr1KO* spleen compared to WT and *Cr1/2KO* animals (Supplemental Fig. 2).

The Cr1 isoform is the dominant Cr2 gene product on FDC

The two major cell types of the mouse that express the *Cr2* gene are the B cell and the FDC. As described above, the Cr1 and Cr2 proteins are generated from alternative splice isoforms from the *Cr2* gene. As shown previously (Fig.1B) immunoblot analysis of total splenic cell populations (isolated by straining free cells away from the FDC-enriched stromal matrix) for the total *Cr2* gene products using a polyclonal rabbit anti-Cr1/2 antibody demonstrated a much higher quantity of Cr2 versus Cr1. A similar pattern is also obtained from the analysis of purified $B220^+$ B cells. FACS analysis of B cells with saturating levels of the Cr1-specific antibody (8C12) in contrast to antibodies recognizing both Cr1 and Cr2 (7G6, 7E9, eBio8D9) also demonstrates that the MFI of Cr2 staining is much higher than that of Cr1 (data not shown). These data, in total, suggest that the predominant isoform of the *Cr2* gene expressed by B cells is the Cr2 protein. Additionally immunohistochemical staining for Cr1 (Cr1-specific antibody clone 8C12) of splenic or lymph node cross-sections has been used by many investigators to definitively mark FDCs. This suggested to us that FDC expression of Cr1 is not equal to B cell expression and that the Cr1 to Cr2 ratio may not be equal in these two cell types. In light of these observations we chose to definitively delineate *Cr1/2* expression in FDC and B cells.

Initially we utilized the same immunohistochemical staining strategy as others to screen splenic cross sections from the *Cr1KO* mice. As shown (Fig. 5A) staining WT, *Cr1KO* and *Cr1/2KO* spleen sections with the anti-Cr1 (CD35) antibody 8C12 demonstrates strong Cr1 expression on the FDC of the WT mice, but an absence of Cr1 expression on the two mouse mutant strains. Thus the *Cr1KO* also shows the expected loss of Cr1 expression by FDC. Staining of parallel sections with an antibody that recognizes both Cr1 and Cr2 (CD21/35) (antibody 7E9) demonstrated a virtually identical pattern of B cell staining evident in the WT and *Cr1KO* sections that was absent from the *Cr1/2KO* section (Fig. 5B). This staining however did not highlight the FDC in the WT sample in a similar fashion as that with the anti-Cr1 antibody.

To further evaluate this question, quantitative RT-PCR and immunoblot analysis was performed on dissociated total unstrained spleen samples from bone marrow transplant experiments in which hematopoietic cells from *Cr1/2KO* mice were transplanted into lethally irradiated WT host mice (*Cr1/2KO*→WT), as well as WT→WT, WT→*Cr1/2KO*, and *Cr1/2KO*→*Cr1KO*. Total replacement of the hematopoietic lineage of host mice with, or without, donor *Cr1/2KO* B cells was confirmed by FACS, and all mice were found to have less than one percent B cells expressing the host Cr1/2 phenotype (Fig. 6A). Transcript analysis from these chimeric mice revealed that the *Cr1* isoform is more highly expressed than that of *Cr2* in the *Cr1/2KO*→WT chimera ($p<0.001$, Fig. 6B). This was in contrast to WT→*Cr1/2KO* and WT→WT, both of which did not display a significant difference in the expression of *Cr1* versus *Cr2*. It should be noted that although some *Cr1/2* transcript is detected in *Cr1/2KO* mice using primers common to both *Cr1/2* this is a distal portion of the transcript (3') that cannot be translated into any portion of Cr1 or Cr2 (12). Comparison of the ratio of relative *Cr1* transcript to *Cr2* transcript demonstrated that the *Cr1/2KO*→WT chimera, in which only FDCs transcribe the *Cr2* locus, expresses *Cr1* about 3.5 times as much as *Cr2*. This is in contrast to the significantly lower 1:1 ratio displayed by the WT→*Cr1/2KO* and WT→WT chimeras, in which B cells are the most common cell type expressing the *Cr2* locus ($p<0.001$ and $p<0.01$ respectively, Fig. 6C). Western blot analysis of total spleen lysate (inclusive of both B cells and FDC) from the same reconstituted mice revealed that Cr1 is nearly the exclusive product of the *Cr2* gene by FDC in that WT irradiated mice reconstituted with *Cr1/2KO* bone marrow primarily express the Cr1 protein (Fig. 6D, left panel). In contrast, Western blot analysis of total spleen lysates from either irradiated WT or *Cr1/Cr2KO* hosts given WT bone marrow transplants shows that the Cr2 protein is the predominant product of B cells (Fig. 6D, left panel). Interestingly, although

Cr1 and *Cr2* transcript data suggests that FDC in the *Cr1/2KO→Cr1KO* chimeras produce only *Cr2* transcript, this transcript was not translated by FDC into appreciable levels of Cr2 protein in contrast to the Cr2 protein produced by the *Cr1KO* B cells: see Fig. 1B,C. For comparison, total splenic lysates from *Cr1/2KO* and WT animals are shown (Fig. 6D, right panel).

Immunoblot analysis for Cr1/2 was also performed on lymph node and spleen lysates from mice 2 days post irradiation. Such peripheral immune organs are virtually devoid of B cells two days after irradiation (data not shown). Spleens were disrupted, single cells were strained away from the splenic matrix, and the resulting matrix material was solubilized in RIPA detergent for immunoblot analysis. As shown in Fig. 6D,center panel, the irradiated splenic tissue matrix was highly enriched for the Cr1 protein as opposed to the Cr2 protein seen in the samples enriched for B cells.

The data detailed above, in total, describe the *Cr1KO* mouse as lacking Cr1 expression on B cells and FDC. Cr2 expression on mouse B cells, though, is very similar to that seen for WT B cells. Additionally, although the Cr2 gene is still transcriptionally active in the FDC of the *Cr1KO* animal, as measured by production of transcripts specific for *Cr2*, there is little to no Cr2 protein expression by these cells (as is also shown for WT FDC which do possess Cr1 protein but not Cr2). These findings suggest that the effect of losing the Cr1 protein in the *Cr1KO* animal is likely to be most pronounced for the functions of the FDC and not the B cell for which the major *Cr2* gene product is the Cr2 protein.

Antibody deficiencies of Cr1KO mice

To identify possible effects of Cr1 deficiency on humoral immunity we measured the quantities of total and antigen specific antibodies of IgM, IgG1, IgG2b, IgG2c, and IgG3 in naïve and immunized mice. The levels of circulating antibodies in naïve *Cr1KO* animals were compared to that of WT and the *Cr1/2KO* animals. As shown (Fig. 7) the levels of circulating IgGs and IgM in the *Cr1KO* animal are not significantly different than that of WT. However, the *Cr1KO* mice (as well as WT) have statistically higher levels of IgG2b, IgG2c and IgG3 than the *Cr1/2KO* mice ($p<0.01$, $p<0.001$, and $p<0.001$ respectively).

Within the naïve antibody repertoire is a collection of immunoglobulins (IgM isotype) known as natural antibodies that are specific for conserved epitopes often found on apoptotic cells and pathogens. Many epitopes recognized by natural antibody have been identified such as phosphorylcholine, chitosan/chitin, and dsDNA. To test Cr1 deficiency on production of natural antibody we quantified the titers of IgM specific for phosphorylcholine, chitosan/chitin, or dsDNA in the serum of naïve mice. Anti-phosphorylcholine antibody was found at significantly reduced titers in *Cr1KO* mice compared to WT mice ($p<0.05$) in a similar magnitude to the reduction seen in *Cr1/2KO* mice ($p<0.001$, Fig. 8A). This pattern of natural antibody deficiency was not the same for anti-chitosan/chitin and anti-dsDNA natural antibodies. Anti-chitosan/chitin antibodies from the *Cr1KO* animals were equivalent to WT levels (but statistically reduced in the *Cr1/2KO* mice) (Fig. 8B), while natural antibodies specific for dsDNA were statistically reduced in the *Cr1KO* mice compared to WT and the *Cr1/2KO* mice (Fig. 8C).

Antigens are generally split into one of three categories defined by the secondary signal that tunes B cell activation upon BCR cross-linking: T-independent 1 (TI-1) provided by Toll-like receptor ligands, TI-2 provided by large repetitive antigens such as polysaccharides, and T-dependent (TD) provided by coincident recognition of protein antigen by CD4 T cells. To test the contribution of Cr1 in antibody responses to such antigens, we immunized *Cr1KO*, WT, and the *Cr1/2KO* mice with the model antigens TNP-LPS (TI-1), DNP-Ficoll (TI-2), or

TNP-KLH (TD), and quantified the antigen specific response of different isotypes of immunoglobulin.

The *Cr1KO* mice generated similar antibody responses to the TI-1, TI-2, and the low dose of TD antigen relative to WT mice (Fig. 9A and Supplemental Fig. 3). In contrast *Cr1/2KO* were generally determined to have lower detectable levels of immunoglobulin against the TI-2 and low dose TD antigen than WT mice as previously observed. A similar reduction for the *Cr1KO* and *Cr1/2KO* animals was observed for the antigen specific IgG3 isotype in response to high dose TNP-KLH immunization (days 7, 14, and 21). Intriguingly both the *Cr1KO* and *Cr1/2KO* mice displayed a significant depression in antigen specific IgM following high dose TNP-KLH for days 7,14 and 21, but a significant expansion of antigen specific IgM (compared to WT) following the day 21 boost with TNP-KLH.

Follow up analysis of immunoglobulin produced against the KLH carrier of the TNP-KLH hapten-carrier conjugate demonstrated a reduction in antigen specific IgM produced by *Cr1KO* and *Cr1/2KO* mice although the levels of antigen specific IgG to KLH in the *Cr1KO* animal was very similar to that of WT (Fig. 9B). The *Cr1KO* animal responses to immunization with whole sheep red blood cells (SRBC) also tracked similarly to WT animals (both IgM and IgG) while the SRBC-specific IgG response of the *Cr1/2KO* animal was significantly less than that of WT (Fig. 9C).

The generation of activated germinal center B cells is reduced in Cr1KO mice

Due to the altered response to the T cell dependent antigen in the Cr1KO mice, we questioned if GC B cells were effectively activated in such mice. To test this we immunized mice with 2×10^8 SRBC and used FACS to assay splenic B cells for activated GC B cell markers. Activated GC B cells are identified by elevated expression of Fas and reduced expression of IgD, as well as increased expression of the glycan epitope recognized by the antibody clone GL7 (3, 33–35). *Cr1KO*, WT and *Cr1/2KO* mice were immunized with SRBC and their spleens isolated 7 days later. Splenocytes were $B220^+$ FACS sorted for B cells and then were identified as GC B cells by IgD^{int} Fas^+. Similar to *Cr1/2KO* mice, *Cr1KO* mice consistently possessed a significantly ($p<0.001$) reduced population of GC B cells in response to SRBC immunizations than WT mice (Fig. 10A, B). GL7 expression was equivalent in the varying IgD^{int} Fas^+ populations indicating that when GC cells were activated in the *Cr1KO* mouse (and *Cr1/2KO* animal) that the level of activation was equivalent to WT (data not shown). To determine if the lack of activated GC B cells in the *Cr1KO* (and *Cr1/2KO*) animals was complement (C3) dependent, we analyzed the generation of GC B cells in SRBC-immunized C3 deficient animals. As shown in Supplemental Fig. 4, *C3KO* mice generated significantly reduced GC B cell populations. However, the small subset of cells from the *C3KO* animal that did gate in the activated GC population also expressed elevated levels of GL7 (data not shown). Therefore the full activation of GC B cells requires C3 in addition to the expression of the Cr1 protein.

Cr2 sufficiency rescues Cr1KO mortality during Streptococcus pneumoniae infection

Cr1/2KO mice generate a deficient primary immune response to the pathogen *S. pneumoniae* and a subsequent poor secondary immune response to infection. To determine if the susceptibility of *Cr1KO* mice to *S. pneumoniae* was similar to that of the *Cr1/2KO* animal (along with WT controls), mice were immunized with 10,000 heat-killed *S. pneumoniae* and infected, ten days later, with 1000 CFU of live bacteria. Survival of *Cr1KO, Cr1/2KO, C3KO*, and WT was statistically analyzed by the Logrank test ($p<0.01$) and revealed that the survival of the *Cr1KO* mice (85%, 2 days post infection (dpi)) was not significantly less than the 100% survival of WT mice (Fig. 11). In contrast to the *Cr1KO* animals, the *Cr1/2KO* mice were significantly ($p<0.05$, 55%, 3dpi) more susceptible to

mortality from the infection. Consistent with the critical role of the complement cascade in control of *S. pneumoniae* infections, none of the *C3KO* mice survived beyond 3 dpi.

Discussion

The complement pathway is a critical component of the innate and acquired immune response. The generation of antibody responses, both T cell dependent and independent, has been demonstrated to be influenced by complement products and their cellular receptors. Animals lacking the *Cr2* gene products, the Cr1 and Cr2 receptors, have defined deficiencies in antibody responses (both natural as well as the result of specific immunizations), heightened sensitivity to bacterial pathogens such as *Steptoccoccus pneumoniae* and a lack of optimal B cell activation(12, 13). The *Cr2* gene is transcriptionally active in B cells and FDC and, via alternative splicing, creates the transcripts specific for Cr1 and Cr2. Gene knockout strategies in the past have eliminated the ability of B cells and FDC to make any of the Cr2 gene products, and thus it has been impossible to delineate the specific functions of either of the individual proteins. In this study we describe the creation of a new mouse line, the *Cr1KO* mouse, in which the exons unique to the Cr1 protein have been deleted by targeted homologous recombination, creating a gene very similar to that of human CR2, which possesses the vestiges of the Cr1-like exons but only produces the CR2 protein (36).

The characterization of the *Cr1KO* animal led us to focus upon Cr1 and Cr2 protein production by B cells and FDC. It had always been a question why immunostaining of splenic germinal centers with an antibody specific for Cr1 identified FDC while similar staining with an antibody that recognizes both Cr1 and Cr2 (there are no specific anti-Cr2 antibodies) primarily identifies B cells (Fig. 5). By teasing apart the protein contributions of the *Cr2* gene in B cells and FDC, we found that the *Cr2* gene product produced in FDC is almost exclusively that of Cr1, while B cells primarily splice to form the Cr2 protein (Fig. 6). Even when the *Cr2* gene is forced to only splice to the Cr2 isoform in the *Cr1KO* animal, the quantity of Cr2 produced by FDC is minimal (*Cr1/2KO→Cr1KO* bone marrow chimera) while that of B cells is normal (Fig. 6D). Thus the deficiency of the *Cr1KO* animal could be expected to have a greater impact upon FDC functions rather than B cell activation/antigen acquisition. Previously Fang et al (37) reported that the *Cr1/2KO* animal reconstituted with bone marrow from either a WT animal or the *Cr1/2KO* would not reconstitute immune complex binding to the germinal centers implicating the role of the *Cr2* gene encoded proteins expressed by FDC to be critical in immune complex retention.

The comparison of antibody titers in naïve and immunized mice of the *Cr1KO* and the *Cr1/2KO* condition demonstrated a more dramatic deficiency when both Cr1 and Cr2 are absent (Fig's. 7,8,9). While the naïve *Cr1/2KO* animal has depressed circulating levels of total IgG2b, IgG2c and IgG3, the *Cr1KO* titers for these antibody types are virtually identical to WT. The responses to both T independent and dependent immunizations generally demonstrated a greater defect for the *Cr1/2KO* than the *Cr1KO* mouse. This is particularly true for the TI-2 antigen DNP-Ficoll, which induced a response equal to WT for the *Cr1KO*.

The greatest variation from WT for the *Cr1KO* animal was evident in the high dose (100μg TNP-KLH) when anti-TNP titers were analyzed (Fig. 9A). *Cr1KO* mice exhibited a reduced production of TNP-specific IgM during the primary immune response, which was similar to the reduction seen in the *Cr1/2KO* mice. Intriguingly both the *Cr1KO* and *Cr1/2KO* animals exhibited significantly elevated levels of TNP-specific IgM compared to WT following the boost of antigen (day 21) in the high dose immunization experiment. The analysis of IgG isotypes from such immunized *Cr1KO* animals was less dramatic. Anti-TNP IgG3 was found to be significantly reduced during the primary response of the *Cr1KO* mouse while

the IgG1, IgG2b, and IgG2c isotypes were not significantly reduced compared to WT. In general the antibody response data for TD antigens from the *Cr1KO* animal suggests a deficiency (compared to WT) in primary activation (demonstrated by the reduced IgM/IgG3 responses) and depressed levels of isotype switching (evidenced by the enhanced production of IgM following the secondary boost).

The generation of antigen specific IgM and IgG responses to the KLH carrier protein or to immunizations with SRBC were intermediate for the *Cr1KO* animal compared to those responses of WT and the *Cr1/2KO* mouse suggesting that the presence of the Cr2 protein on B cells in the *Cr1KO* animal partially mitigated the Cr1 deficiency (Fig. 9B,C). These results may vary from the anti-TNP responses noted above in that the population of responding B cells is much more limited for the TNP response than the response to the many epitopes provided by the KLH protein and SRBC. Clearly the lack of both Cr1 and Cr2 proteins dramatically depressed the IgG anti-SRBC response which was virtually identical to WT in the *Cr1KO* mouse. However, the depressed anti-KLH and anti-SRBC IgM responses in both the *Cr1KO* and *Cr1/2KO* animal lines, compared to WT, suggests that Cr1, expressed by either B cells or FDC, may be playing a role in this initial antigen response. Previous work on an independently generated Cr1 and Cr2 deficient mouse by Molina *et al.* (13) also described SRBC-specific IgM primary responses very similar to those demonstrated in our studies in this report.

Our IgG analysis of the *Cr1KO* animal may also be compared to bone marrow chimera studies in which antibody responses have been analyzed with animals lacking functional *Cr2* gene expression in either bone marrow lineages or the FDC. One such study analyzed responses to immunization with SRBC and KLH showing that while the absence of *Cr2* gene products expressed by FDC had a profound impact upon antibody generation that the generation of an optimal response also needed B cell *Cr2* gene products (37). The demonstration of the predominance of expression of Cr1 on FDC would suggest that the IgG response to SRBC or KLH in the *Cr1KO* mice should mirror those of bone marrow chimeras in which complement receptor expression is limited to B cells as described in that report. Our data on the IgG responses to SRBC immunization demonstrate there is not a significant difference in response to these immunogens, suggesting that bone marrow chimeras may not perfectly define the phenotype of Cr1 deficiency. Further, despite the lack of significance between the *Cr1KO* and WT IgG responses to SRBC the similarity of the pattern of the IgG responses to KLH by *Cr1KO* mice relative to WT and *Cr1/2KO* mice (Fig. 9B,C, right panels) suggests these differences are more than random variation. A more recent bone marrow chimera analysis (using Cr1/2 deficiency bred upon a BALB/c background) demonstrated that the presence or absence of *Cr2* gene products on B cells did not alter the generation of various IgG isotypes to immunizations with SRBC, but that *Cr2* gene expression by FDC was critical for such responses (14). Intriguingly this study also demonstrated that immunization with IgM-SRBC complexes required Cr2 gene products on both B cells and FDC for optimal antibody responses. Our data generated with the *Cr1KO* animal fundamentally agrees with the conclusions reached by Rutemark and colleagues(14) in that the ability of B cells to efficiently class switch from IgM to IgG isotypes (whether they express *Cr2* gene products or not) is compromised in the absence of the Cr1 protein expressed by the FDC. There are, however, specific points of variance between our studies and those utilizing bone marrow chimera models that may be a consequence of the experimental procedures. For example, bone marrow chimera studies require irradiation and bone marrow reconstitution that may result in an immune environment that is not functionally equivalent to the environment found in a non-irradiated animal (in our case, the *Cr1KO* line). Additionally in removing the ability of B cells to produce the Cr1 protein in the *Cr1KO* animal, all *Cr2* gene transcripts are committed to producing the Cr2 protein which is evidenced in the elevated MFI of Cr2 expression by B cells of the *Cr1KO* mouse

compared to WT. This increase in Cr2 protein may heighten the sensitivity of the activation of B cells, reducing a difference between the *Cr1KO* and WT. Alternatively Cr1 expressed by B cells may suppress B cell activation. Mouse strain differences may also play a role in that our antibody analyses, and those of Fang et al (37), used the C57BL/6 background while those of Rutemark (14) used the BALB/c background. Previously we have found that the *Cr1/2KO* deficiency on a BALB/c background created a more inflamed splenic environment than the same deficiency on a C57BL/6 background that may also alter antibody responses (25). Finally, a previous report had suggested that some of the functional defects in B cell responses in the *Cr1/2KO* animal was due to the elevated surface expression of CD19, usually found in a complex with Cr1/2, CD81 and Ifitm1/3 (17), leading to anergic responses. The bone marrow chimera models described above utilizing marrow reconstitution from the *Cr1/2KO* mouse thus possess B cells expressing elevated levels of CD19. However, the analysis of B cells obtained from the *Cr1KO* animal showed a lower level of CD19 than WT thus mitigating the concerns of CD19-dependent B cell anergy in the *Cr1KO* mouse.

The generation of activated GC B cells requires the interaction of the antigen specific B cell with antigen and the cognate T cell. Previously it had been shown that the number of GC B cells after immunization were reduced in *Cr1/2KO* mice (38), which was presumed to be due, in part, to the loss of Cr2 signaling on the B cell as part of the BCR co-receptor complex. Interestingly, we found that the *Cr1KO* animal also does not generate activated B cells (Fig. 10) based upon the IgD and Fas expression status (Fig. 10). Indeed the immunized *Cr1KO* and *Cr1/2KO* animals had the equivalent percentages of activated B cells of the unimmunized WT control. The movement of B cells from the region of high B cell proliferation known as the dark zone (DZ) to the FDC localized light zone (LZ) of the germinal center (interzonal migration) has been defined as “cyclic re-entry” in which antigen specific B cells are selected for by binding to antigen held by the FDC followed by encounter with antigen-specific T cells and migration to the DZ for proliferation (39–41). After activation and proliferation in the DZ (accompanied by somatic hypermutation and isotype switching), the antigen-specific B cells then cycle back into the LZ for another round of positive antigen selection on the FDC. The absence of such activated B cells in the *Cr1KO* animal suggests that antigen bound by the FDC Cr1 protein is critical for this pathway to optimally proceed and C3 is a required ligand. Further analysis of bone marrow chimera animals as well as characterization of DZ and LZ associated B cells (via differential expression of CXCR4 and CD83) (42) will help us determine the specific signaling defect associated with the absence of Cr1.

Functions associated with the *Cr2* gene products have also been implicated in the development and progression of systemic lupus erythematosus (SLE) although the specific pathway(s) of Cr1/Cr2 control have not been described (43, 44). The loss of Cr1 on the surface of FDC resulting in the loss of positive selection of activated B cells may allow such cells to escape into the periphery. The mutations in the VDJ region associated with the presence of the B cell in the DZ is random, such that the generation of autoreactive B cells could easily proceed. In fact, the immunoglobulin genes obtained from autoreactive B cells do demonstrate a high level of VDJ somatic hypermutation (43–46). If the absence of the Cr1 expression by the FDC allows such cells to exit the germinal center without selection, then the dissemination of autoreactive B cells into the periphery of the animal may be enhanced. Experiments to test this hypothesis are currently underway.

In summary, these data provide two new findings in support of the model that expression of *Cr2* gene products by FDC and B cells is required for optimal antigen-specific B cell activation and antibody production to T-dependent antigens: one, the novel discovery that Cr1 is preferentially expressed by FDC while Cr2 is preferentially expressed by B cells, and

two, that Cr1 is more integral to germinal center B cell activation and response to T-dependent antigens than T-independent responses. The similarity and differences between deletion of Cr1 alone or Cr1/2 together highlights the importance and functional independence of these similar proteins, and emphasizes the significance of the new *Cr1KO* mouse line. These findings are relevant for the optimization of adjuvants targeted to FDCs for the enhancement of humoral immunity (47).

Supplementary Material

Refer to Web version on PubMed Central for supplementary material.

Acknowledgments

We thank the members of the combined Weis labs for their helpful discussions and critical review of the data, and specifically thank Peter Pioli for assistance in western blots. We thank the Utah Transgenic and Knockout Core facility (Dr. Susan Tomowski) for the assistance in generating the Cr1KO animal, and the Flow Cytometric Core facility for their assistance in cell analysis.

Abbreviations

Cr1	Complement receptor 1
Cr2	Complement receptor 2
Cr1KO	Cr1 knockout mouse
Cr1/2KO	Cr1 and Cr2 knockout mouse
C3KO	complement component C3 knockout mouse
FDC	follicular dendritic cells
GC	germinal center
BCR	B cell receptor
MAC	membrane attack complex
FOB	follicular mature B cells
MZB	marginal zone B cells
SRBC	sheep red blood cells
LZ	light zone
DZ	Dark Zone
SLE	systemic lupus erythematosus

Literature Cited

1. Xu Z, Zan H, Pone EJ, Mai T, Casali P. Immunoglobulin class-switch DNA recombination: induction, targeting and beyond. Nat Rev Immunol. 2012; 12:517–531. [PubMed: 22728528]
2. Vinuesa CG, Linterman MA, Goodnow CC, Randall KL. T cells and follicular dendritic cells in germinal center B-cell formation and selection. Immunol reviews. 2010; 237:72–89.
3. Wang X, Cho B, Suzuki K, Xu Y, Green JA, An J, Cyster JG. Follicular dendritic cells help establish follicle identity and promote B cell retention in germinal centers. J Exp Med. 2011; 208:2497–2510. [PubMed: 22042977]
4. Ferguson AR, Youd ME, Corley RB. Marginal zone B cells transport and deposit IgM-containing immune complexes onto follicular dendritic cells. Int Immunol. 2004; 16:1411–1422. [PubMed: 15326094]

5. Gonzalez SF, Degn SE, Pitcher LA, Woodruff M, Heesters BA, Carroll MC. Trafficking of B Cell Antigen in Lymph Nodes. Annu Rev Immunol. 2011; 29:215–233. [PubMed: 21219172]
6. Suzuki K, Grigorova I, Phan TG, Kelly LM, Cyster JG. Visualizing B cell capture of cognate antigen from follicular dendritic cells. J Exp Med. 2009; 206:1485–1493. [PubMed: 19506051]
7. Walport MJ. Complement. N Engl J Med. 2001; 344:1058–1066. [PubMed: 11287977]
8. Ricklin D, Hajishengallis G, Yang K, Lambris JD. Complement: a key system for immune surveillance and homeostasis. Nat Immunol. 2010; 11:785–797. [PubMed: 20720586]
9. Walport MJ. Complement. N Engl J Med. 2001; 344:1140–1144. [PubMed: 11297706]
10. Pepys MB. Role of complement in induction of antibody production in vivo. Effect of cobra factor and other C3-reactive agents on thymus-dependent and thymus-independent antibody responses. J Exp Med. 1974; 140:126–145. [PubMed: 4545894]
11. Carroll MC, Isenman DE. Regulation of humoral immunity by complement. Immunity. 2012; 37:199–207. [PubMed: 22921118]
12. Haas KM, Hasegawa M, Steeber DA, Poe JC, Zabel MD, Bock CB, Karp DR, Briles DE, Weis J, Tedder TF. Complement receptors CD21/35 link innate and protective immunity during Streptococcus pneumoniae infection by regulating IgG3 antibody responses. Immunity. 2002; 17:713–723. [PubMed: 12479818]
13. Molina H, Holers VM, Li B, Fung Y, Mariathasan S, Goellner J, Strauss-Schoenberger J, Karr RW, Chaplin DD. Markedly impaired humoral immune response in mice deficient in complement receptors 1 and 2. Proc Natl Acad Sci U S A. 1996; 93:3357–3361. [PubMed: 8622941]
14. Rutemark C, Bergman A, Getahun A, Hallgren J, Henningsson F, Heyman B. Complement Receptors 1 and 2 in Murine Antibody Responses to IgM-Complexed and Uncomplexed Sheep Erythrocytes. PLoS ONE. 2012; 7(7):e41968. [PubMed: 22848677]
15. Molina H, Kinoshita T, Webster CB, Holers VM. Analysis of C3b/C3d binding sites andfactor I cofactor regions within mouse complement receptors 1 and 2. J Immunol. 1994; 153:789–795. [PubMed: 8021513]
16. Jacobson AC, Weis JH. Comparative functional evolution of human and mouse CR1 and CR2. J Immunol. 2008; 181:2953–2959. [PubMed: 18713965]
17. Haas KM, Poe J, Tedder TF. CD21/35 promotes protective immunity to Streptococcus pneumoniae through a complement-independent but CD19-dependent pathway that regulates PD-1 expression. J Immunol. 2009; 183:3661. [PubMed: 19710450]
18. Marchbank KJ, Watson CC, Ritsema DF, Holers VM. Expression of human complement receptor 2 (CR2, CD21) in Cr2-/-mice restores humoral immune function. J Immunol. 2000; 165:2354–2361. [PubMed: 10946257]
19. Pappworth IY, Hayes C, Dimmick J, Morgan BP, Holers VM, Marchbank KJ. Mice expressing human CR1/CD35 have an enhanced humoral immune response to T-dependent antigens but fail to correct the effect of premature human CR2 expression. Immunobiology. 2012; 217:147–157. [PubMed: 21783272]
20. Bunting M, Bernstein KE, Greer JM, Capecchi MR, Thomas KR. Targeting genes for self-excision in the germ line. Genes Dev. 1999; 13:1524–1528. [PubMed: 10385621]
21. Zabel MD, Weis JJ, Weis JH. Lymphoid transcription of the murine CD21 gene is positively regulated by histone acetylation. J Immunol. 1999; 163:2697–2703. [PubMed: 10453011]
22. Debnath I, Roundy KM, Weis JJ, Weis JH. Defining in vivo transcription factor complexes of the murine CD21 and CD23 genes. J Immunol. 2007; 178:7139–7150. [PubMed: 17513763]
23. Morrison TB, Ma Y, Weis JH, Weis JJ. Rapid and sensitive quantification of Borrelia burgdorferi-infected mouse tissues by continuous fluorescent monitoring of PCR. J Clin Microbiol. 1999; 37:987–992. [PubMed: 10074514]
24. Roundy KM, Weis JJ, Weis JH. Deletion of putative intronic control sequences does not alter cell or stage specific expression of Cr2. Mol Immunol. 2009; 47:517–525. [PubMed: 19740539]
25. Jacobson AC, Weis JJ, Weis JH. Complement receptors 1 and 2 influence the immune environment in a B cell receptor-independent manner. J Immunol. 2008; 180:5057–5066. [PubMed: 18354231]

26. Rapaka RR, Ricks DM, Alcorn JF, Chen K, Khader SA, Zheng M, Plevy S, Bengtén E, Kolls JK. Conserved natural IgM antibodies mediate innate and adaptive immunity against the opportunistic fungus Pneumocystis murina. J Exp Med. 2010; 207:2907–2919. [PubMed: 21149550]
27. Koganei A, Tsuchiya T, Samura K, Nishikibe M. Use of whole sheep red blood cells in ELISA to assess immunosuppression in vivo. J Immunotoxicol. 2007; 4:77–82. [PubMed: 18958715]
28. Carlsson F, Getahun A, Rutemark C, Heyman B. Impaired antibody responses but normal proliferation of specific CD4+ T cells in mice lacking complement receptors 1 and 2. Scand J Immunol. 2009; 70:77–84. [PubMed: 19630912]
29. Ray A, Dittel BN. Isolation of mouse peritoneal cavity cells. J Vis Exp. 2010; (35):e1488.
30. Romero-Steiner S, Libutti D, Pais LB, Dykes J, Anderson P, Whitin JC, Keyserling HL, Carlone GM. Standardization of an opsonophagocytic assayfor the measurement of functional antibody activity against Streptococcus pneumoniae using differentiated HL-60 cells. Clin Diagn Lab Immunol. 1997; 4:415–422. [PubMed: 9220157]
31. Ahearn JM, Fischer MB, Croix D, Goerg S, Ma M, Xia J, Zhou X, Howard RG, Rothstein TL, Carroll MC. Disruption of the Cr2 locus results in a reduction in B-1a cells and in an impaired B cell response to T-dependent antigen. Immunity. 1996; 4:251–262. [PubMed: 8624815]
32. Hasegawa M, Fujimoto M, Poe JC, Steeber DA, Tedder TF. CD19 can regulate B lymphocyte signal transduction independent of complement activation. J Immunol. 2001; 167:3190–3200. [PubMed: 11544305]
33. Yoshino T, Kondo E, Cao L, Takahashi K, Hayashi K, Nomura S, Akagi T. Inverse expression of bcl-2 protein and Fas antigen in lymphoblasts in peripheral lymph nodes and activated peripheral blood T and B lymphocytes. Blood. 1994; 83:1856–1861. [PubMed: 7511441]
34. Cervenak L, Magyar A, Boja R, Laszlo G. Differential expression of GL7 activation antigen on bone marrow B cell subpopulations and peripheral B cells. Immunol Lett. 2001; 78:89–96. [PubMed: 11672592]
35. Naito Y, Takematsu H, Koyama S, Miyake S, Yamamoto H, Fujinawa R, Sugai M, Okuno Y, Tsujimoto G, Yamaji T, Hashimoto Y, Itohara S, Kawasaki T, Suzuki A, Kozutsumi Y. Germinal center marker GL7 probes activation-dependent repression of N-glycolylneuraminic acid, a sialic acid species involved in the negative modulation of B-cell activation. Mol Cell Biol. 2007; 27:3008–3022. [PubMed: 17296732]
36. Holguin MH, Kurtz CB, Parker CJ, Weis J, Weis JH. Loss of Human CR1 and Murine Crry-like Exons in Human CR2 Transcripts Due to CR2 Gene Mutations. J Immunol. 1990; 145:1776–1781. [PubMed: 2144008]
37. Fang Y, Xu C, Fu YX, Holers VM, Molina H. Expression of complement receptors 1 and 2 on follicular dendritic cells is necessary for the generation of a strong antigen-specific IgG response. J Immunol. 1998; 160:5273–5279. [PubMed: 9605124]
38. Wu X, Jiang N, Fang YF, Xu C, Mao D, Singh J, Fu YX, Molina H. Impaired affinity maturation in Cr2-/-mice is rescued by adjuvants without improvement in germinal center development. J Immunol. 2000; 165:3119–3127. [PubMed: 10975825]
39. Kepler TB, Perelson AS. Cyclic re-entry of germinal center B cells and the efficiency of affinity maturation. Immunol Today. 1993; 14:412–415. [PubMed: 8397781]
40. Oprea M, Perelson AS. Somatic mutation leads to efficient affinity maturation when centrocytes recycle back to centroblasts. J Immunol. 1997; 158:5155–5162. [PubMed: 9164931]
41. Victora GD, Nussenzweig MC. Germinal centers. Annu Rev Immunol. 2012; 30:429–457. [PubMed: 22224772]
42. Victora GD, Dominguez-Sola D, Holmes AB, Deroubaix S, Dalla-Favera R, Nussenzweig MC. Identification of human germinal center light and dark zone cells and their relationship to human B-cell lymphomas. Blood. 2012; 120:2240–2248. [PubMed: 22740445]
43. Boackle SA, Culhane KK, Brown JM, Haas M, Bao L, Quigg RJ, Holers VM. CR1/CR2 deficiency alters IgG3 autoantibody production and IgA glomerular depositionin the MRL/lpr model of SLE. Autoimmunity. 2004; 37:111–123. [PubMed: 15293881]
44. Boackle SA, Holers VM, Chen X, Szakonyi G, Karp DR, Wakeland EK, Morel L. Cr2, a candidate gene in the murine Sle1c lupus susceptibility locus, encodes a dysfunctional protein. Immunity. 2001; 15:775–785. [PubMed: 11728339]

45. van Es JH, Gmelig Meyling FH, van de Akker WR, Aanstoot H, Derksen RH, Logtenberg T. Somatic mutations in the variable regions of a human IgG anti-double-stranded DNA autoantibody suggest a role for antigen in the induction of systemic lupus erythematosus. J Exp Med. 1991; 173:461–470. [PubMed: 1899104]

46. Mietzner B, Tsuiji M, Scheid J, Velinzon K, Tiller T, Abraham K, Gonzalez JB, Pascual V, Stichweh D, Wardemann H, Nussenzweig MC. Autoreactive IgG memory antibodies in patients with systemic lupus erythematosus arise from nonreactive and polyreactive precursors. Proc Natl Acad Sci U S A. 2008; 105:9727–9732. [PubMed: 18621685]

47. Mattsson J, Yrlid U, Stensson A, Schön K, Karlsson MCI, Ravetch JV, Lycke NY. Complement Activation and Complement Receptors on Follicular Dendritic Cells Are Critical for the Function of a Targeted Adjuvant. J Immunol. 2011; 187:3641–3652. [PubMed: 21880985]

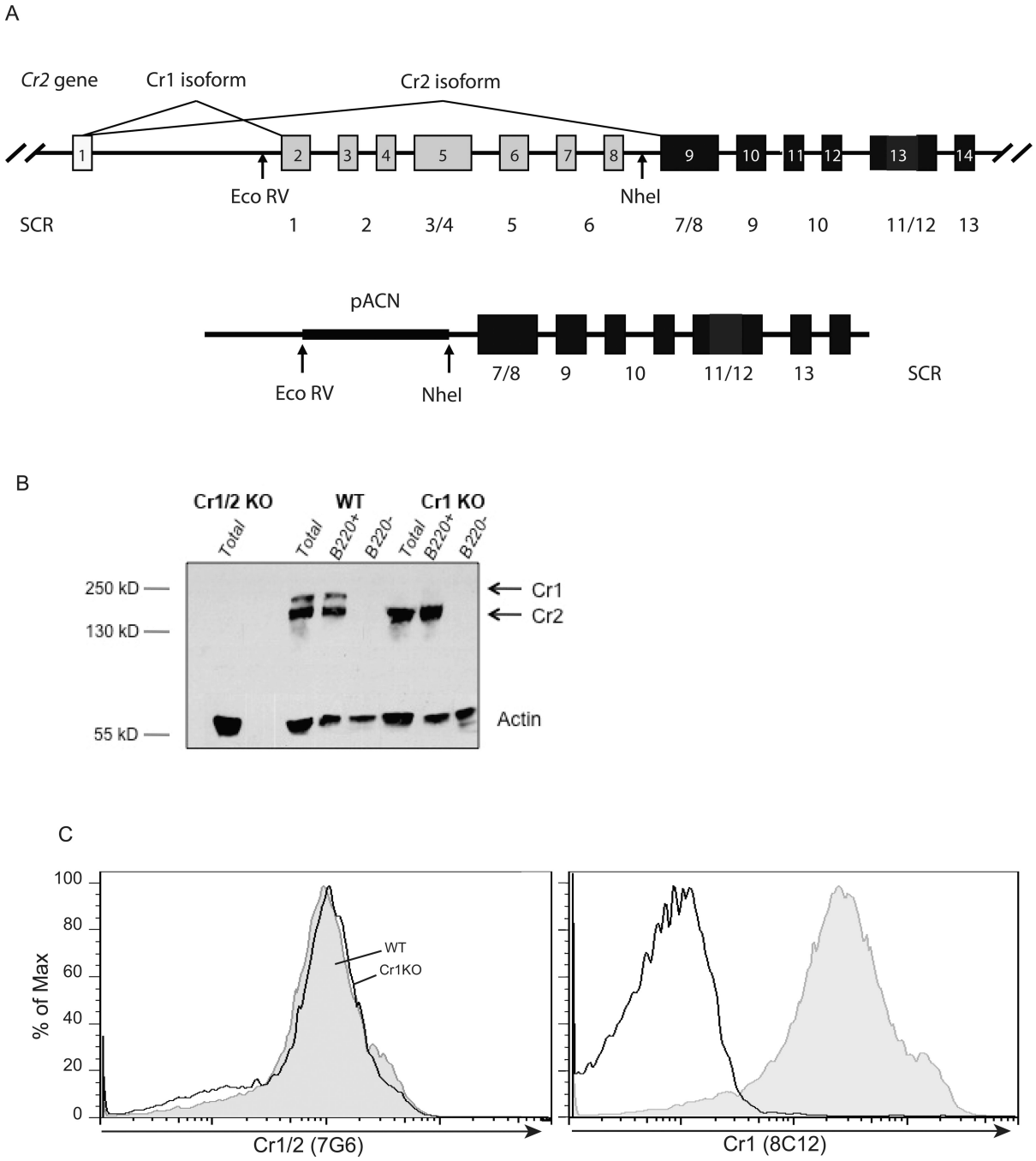

Figure 1.

Cr1 specific deletion by targeted homologous recombination. *A*, Diagram of the *Cr2* gene and the construct used for targeted deletion of the Cr1 specific exons. Exons are denoted 1–14 and not inclusive of all of the 3' *Cr2* gene exons. The coding sequences for the amino terminal SCR domains are also noted with the *Cr1KO* deletion resulting in the deletion of exons encoding the first 6 SCR of the Cr1 protein. *B*, Western Blot analysis of strained spleen lysates (no FDC) from $B220^{+}$ sorted, $B220^{-}$ sorted, or total spleen cells. *C,* FACS analysis of CD19+B220+ mature splenic B cells for the expression of Cr1 and Cr2 (left panel, 7G6 antibody) and Cr1 (right panel, 8C12 antibody).

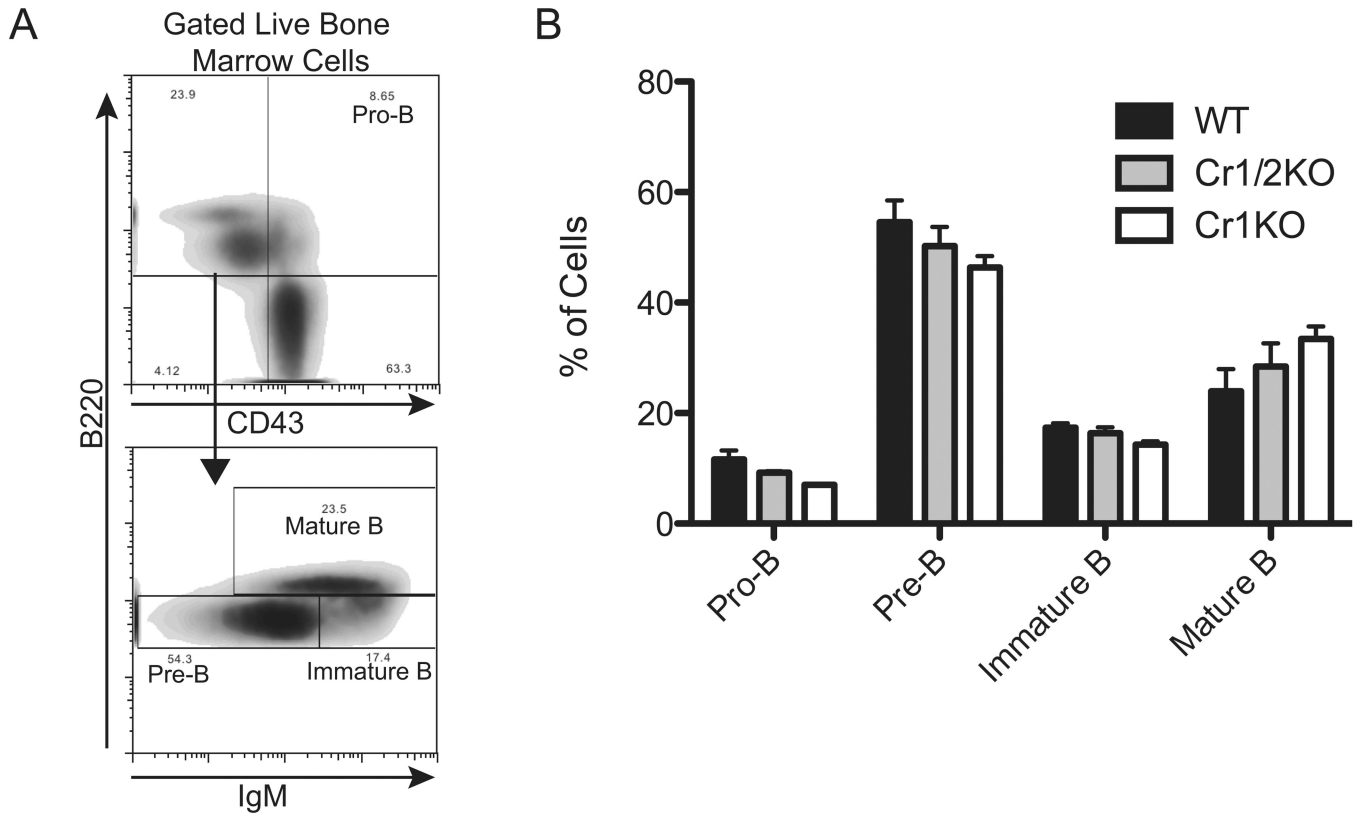

Figure 2.

Analysis of bone marrow B cell populations from WT, *Cr1KO*, and *Cr1/2KO* mice. *A*, Representative gating for delineating pro- ($B220^{+}$ $CD43^{+}$), pre-($CD43^{-}$ IgM^{lo} $B220^{lo}$), immature ($CD43^{-}$ IgM^{hi} $B220^{lo}$) and mature ($CD43^{-}$ IgM^{hi} $B220^{hi}$) B cells. All cells were first segregated as live ($DAPI^{-}$). *B*, Quantification of the frequency of pro-, pre-, immature, and mature B cells from WT, *Cr1/2KO*, and *Cr1KO* bone marrow as defined by the gating strategy in *A*. (Pre-, immature, and mature B cell populations not significantly different by ANOVA). (n=3; age and sex matched 8–12 week old mice; C57Bl/6 background).

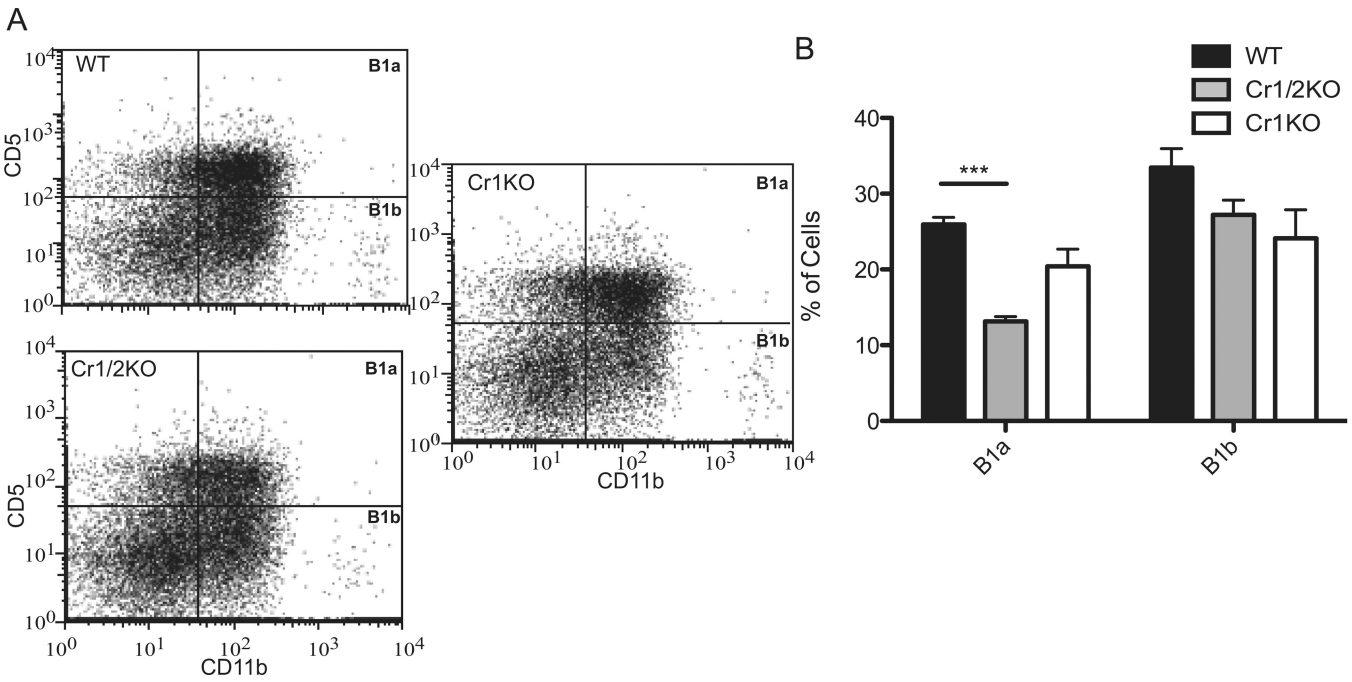

Figure 3.

Analysis of *Cr1KO* peritoneal B1a and B1b populations by FACS. *A*, Representative graphs of B1a ($CD5^+$ $CD11b^+$) and B1b ($CD5^-$ $CD11b^+$) cell population frequency in WT, *Cr1KO*, and *Cr1/2KO* mice. All cells shown were first segregated as live ($DAPI^-$) and $B220^+$. *B*, Quantification of B1a and B1b population frequency (One-way ANOVA $p<0.05$ for B1a; B1b not significantly different). (n=4 WT and *Cr1KO*, n=3 *Cr1/2KO*; age and sex matched 8–12 week old mice; C57Bl/6 background; ***= $p<0.001$ by student's t-test).

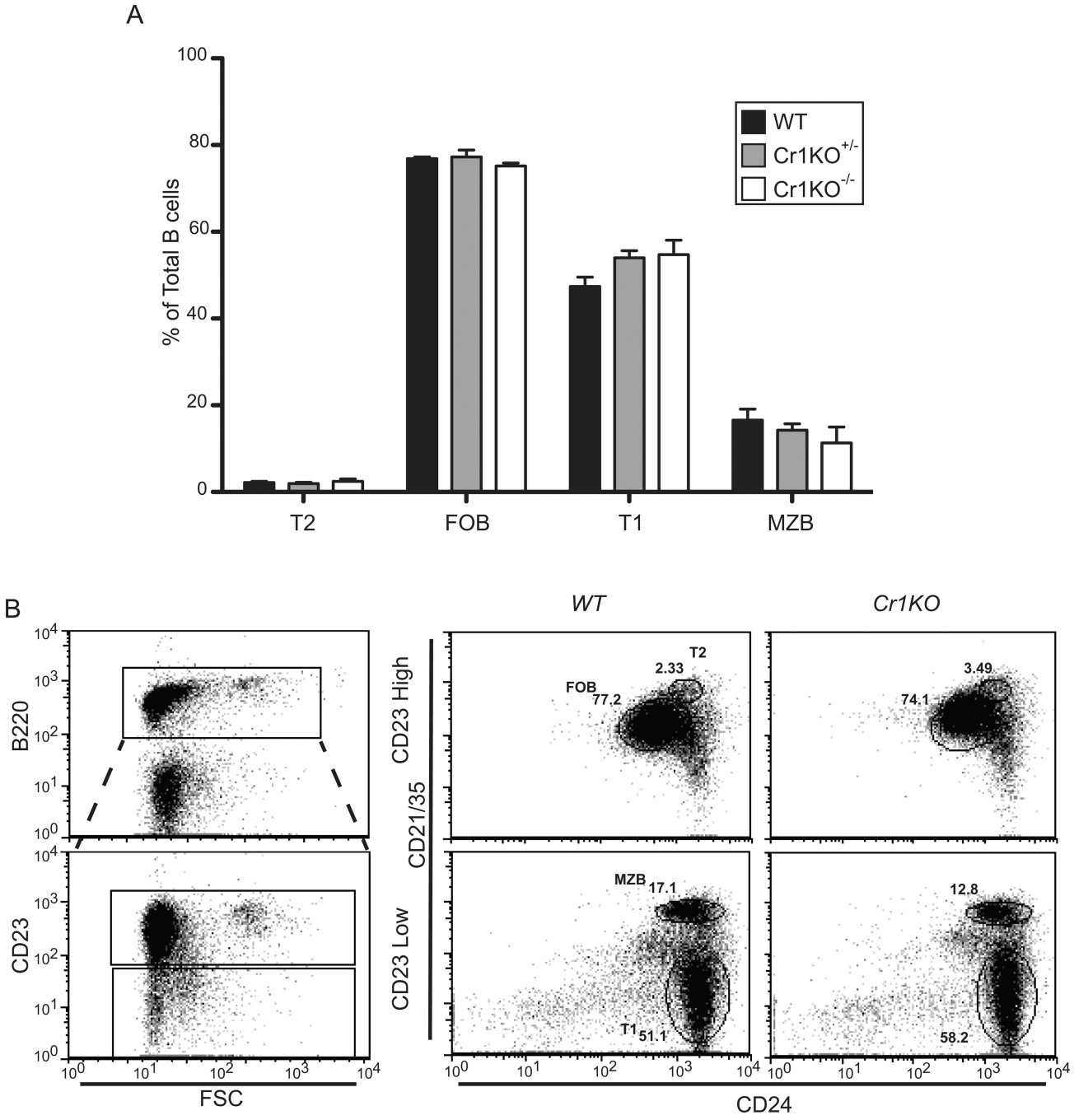

Figure 4.

Analysis of *Cr1KO* splenic B cell populations. *A*, Quantification of transitional 1 (T1), T2, follicular mature (FOB), and marginal zone (MZB) B cell population frequencies in homozygous and heterozygous *Cr1KO* compared to WT mice. Populations were determined by segregating all $B220^{+}$ splenocytes into $CD23^{hi}$ and $CD23^{lo}$ populations and defining the T1, T2, FOB, and MZB B cells by differential expression of CD24 and CD21/35. Representative plots of WT and *Cr1KO* are shown in panel *B*. (n=3 littermates, C57BL/6 background; One-way ANOVA performed on each population set).

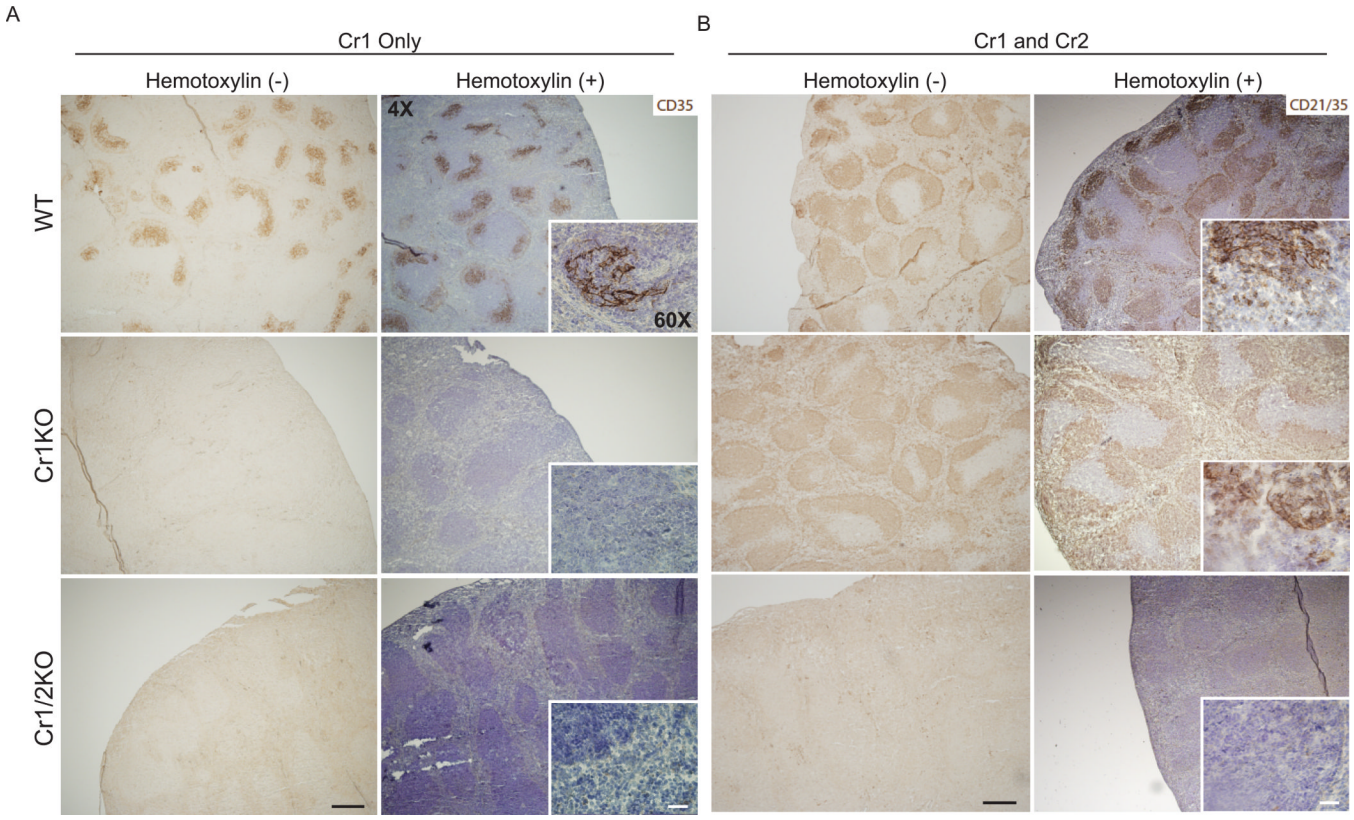

Figure 5.

Immunohistochemistry of Cr1 (CD35) and Cr1/2 (CD21/35) in splenic cross-sections. *A*, Cr1 (CD35) was detected with the monoclonal antibody 8C12, and (*B*) Cr1/2 (CD21/35) were detected using the monoclonal antibody 7E9. Antibody bound Cr1 and Cr1/2 were visualized by horseradish peroxidase reactivity with DAB (brown). Hemotoxylin counterstaining for enhanced visualization of the splenic architecture is shown in blue. (Magnification of all images are at 4X and insets were taken at 60X). Example is from single mice but representative of multiple similar analyses.

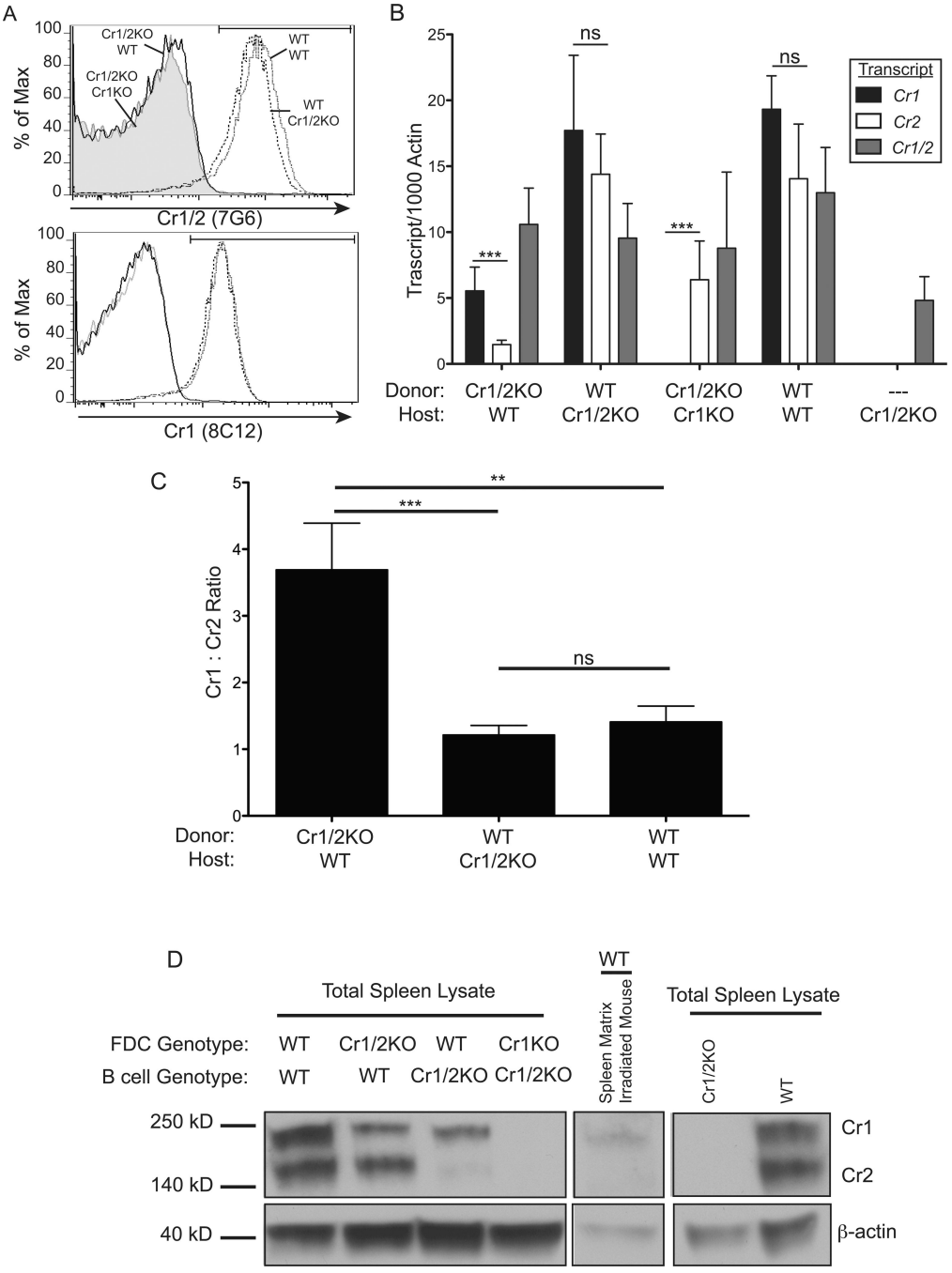

Figure 6.

Quantitative RT-PCR and immunoblot analysis of Cr1 and Cr2 expression on FDC and B cells. *A*, Representative histograms of surface CR1 and CR1/2 on live peripheral blood B220^{+} cells - from WT(donor) →WT(host) (gray line), WT→*Cr1/2KO* (dotted line*),* *Cr1/2KO*→WT (black line), *Cr1/2KO*→*Cr1KO* (gray fill) - demonstrating full engraftment 6 weeks after bone marrow transplant into lethally irradiated mice. *B*, Quantitative RT-PCR analysis of *Cr1* (black bars), *Cr2* (white bars), and *Cr1/2* (gray bars) transcript in total spleen cDNA isolates from bone marrow chimeras. *C*, Ratio of *Cr1*:*Cr2* transcripts quantified in (*B*) from *Cr1/2KO*→WT, WT→*Cr1/2KO*, and WT→WT chimeras. *D*, Immunoblot analysis of the 190kD Cr1 and 140kD Cr2 proteins in total spleen lysates from chimeras (left

panel), a mouse two days post-lethal irradiation (center panel), and control *Cr1/2KO* and WT (right panel). (n=8 *Cr1/2KO*→WT; n=3 WT→*Cr1/2KO*; n=9 *Cr1/2KO*→*Cr1KO*; n=2 WT→WT; n=4 *Cr1/2KO*; error bars represent SEM; ns=not significant, **=p<0.01, ***=p<0.001 by student's t-test) (β-actin was used as a loading control; 40kD).

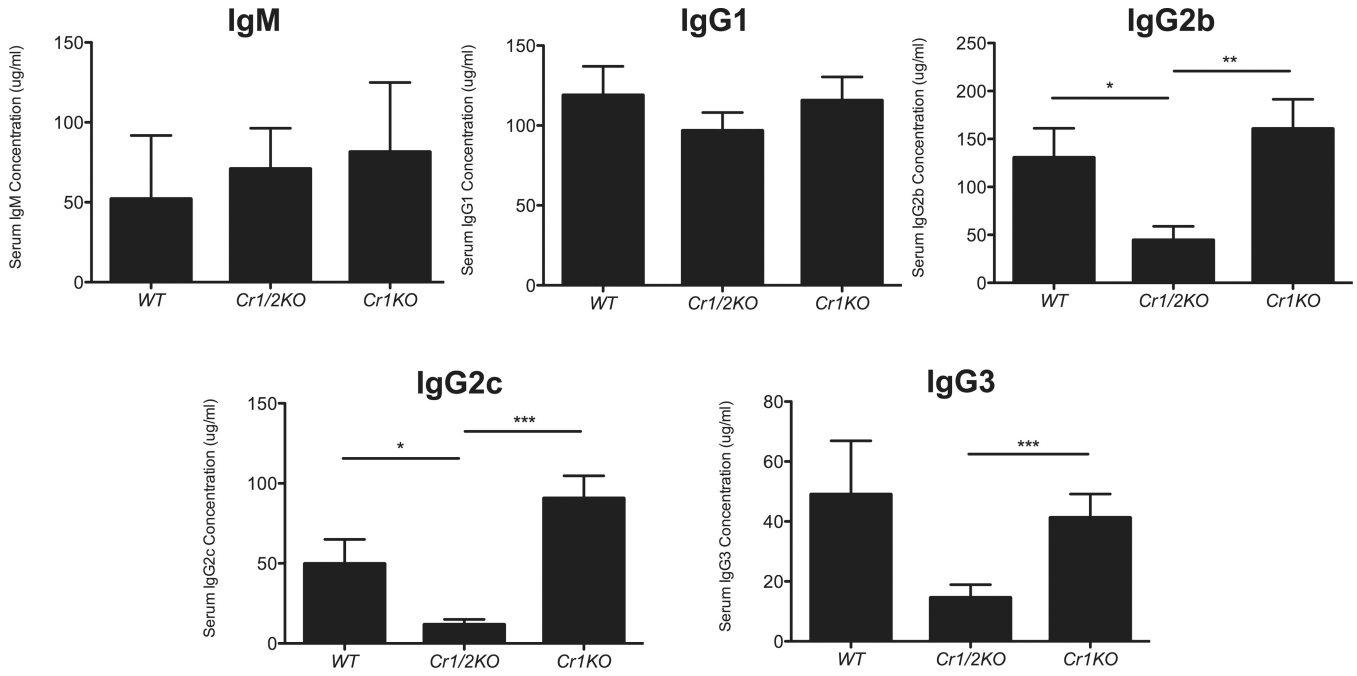

Figure 7.

ELISA quantification of naïve serum immunoglobulin. Concentration of total IgM, IgG1, IgG2b, IgG2c, and IgG3 immunoglobulin isotypes from serum of naïve WT, *Cr1KO*, and *Cr1/2KO* mice. (n=11; 8–16 week old sex matched mice; error bars represent SEM; *=p<0.05, **=p<0.01, ***=p<0.001 by student's t-test).

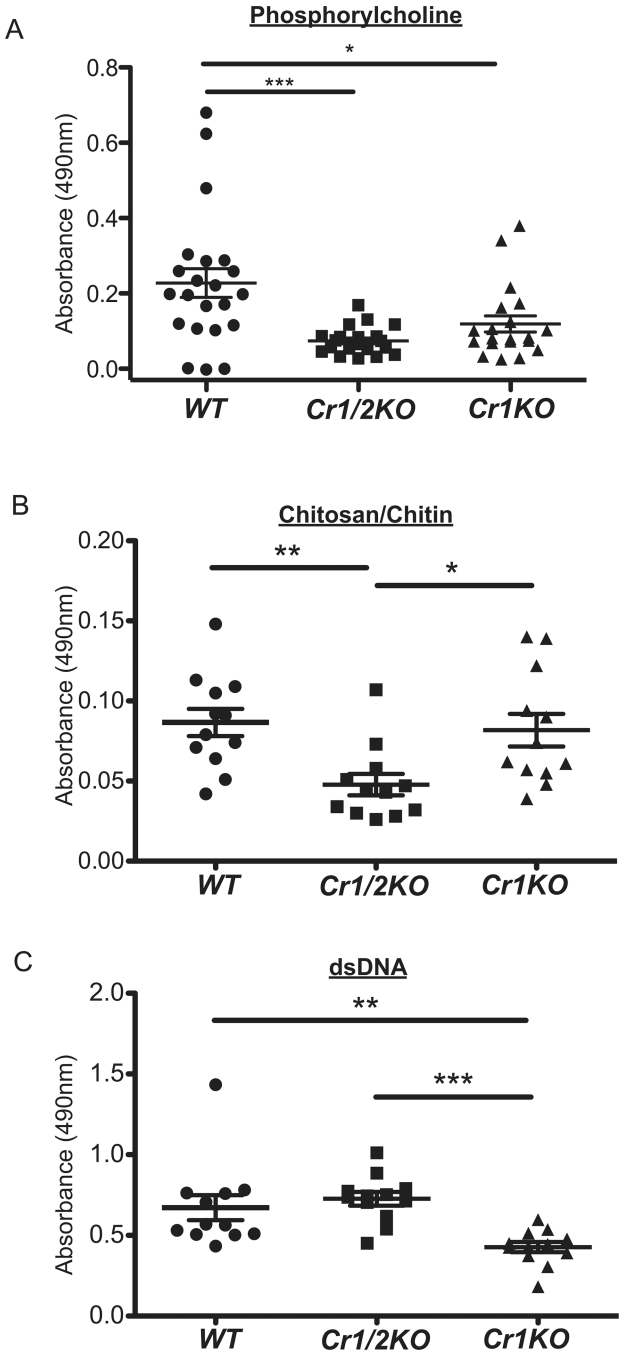

Figure 8.

Circulating natural antibody quantification. Detection of natural antibody (IgM) specific for (*A*) phosphorylcholine, (*B*) chitosan/chitin, and (*C*) dsDNA (calf thymus DNA) determined (see *Materials*) from serum of WT, *Cr1KO*, and *Cr1/2KO* mice. (n=12–22, 8–16 week old sex matched mice; error bars represent SEM; *=p<0.05, **=p<0.01, ***=p<0.001 by student's t-test).

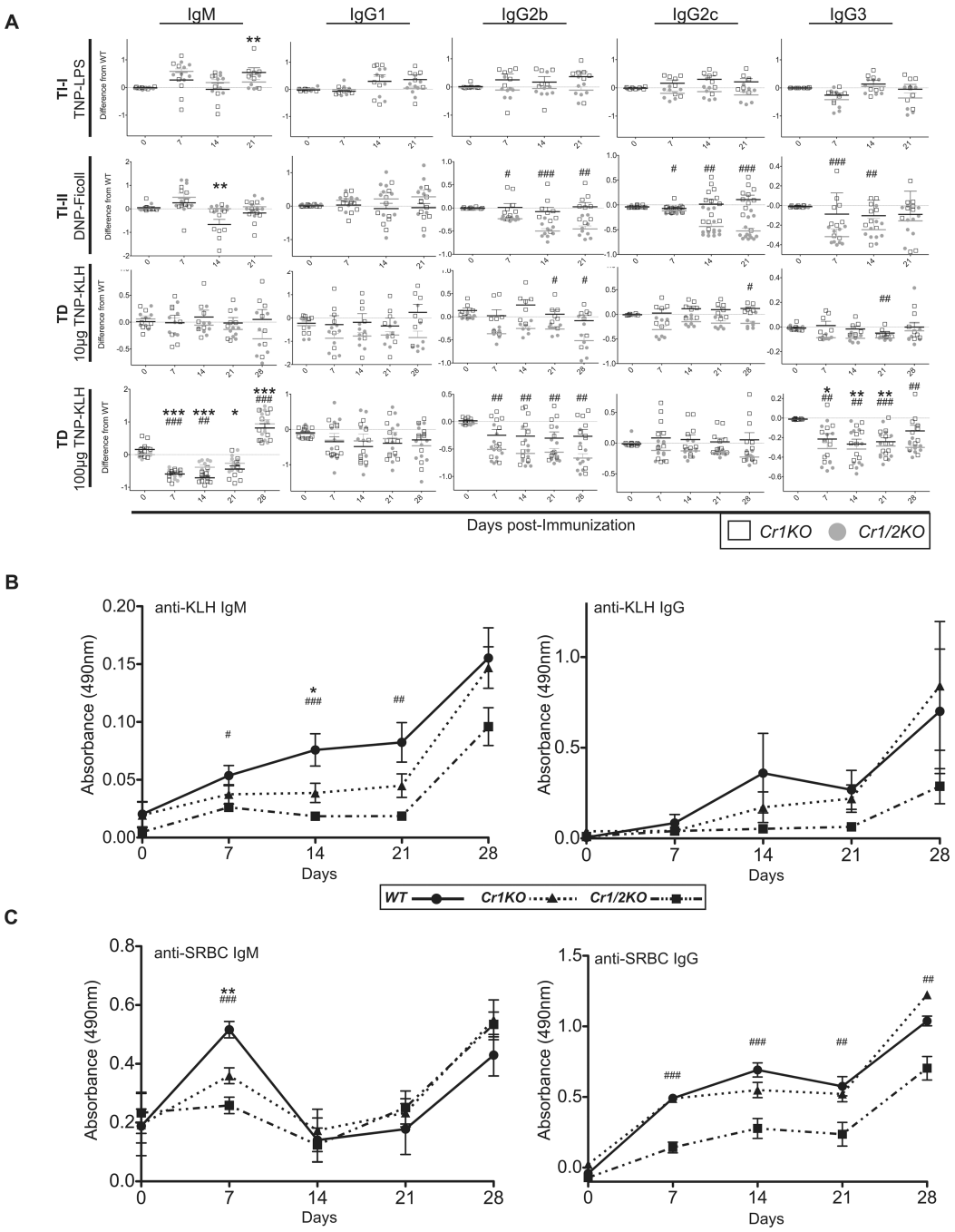

Figure 9.

TI-1, TI-2, and TD antigen specific immunoglobulin response. *A*, Deviation from WT in production of antigen specific immunoglobulin of the isotypes IgM, IgG1, IgG2b, IgG2c and IgG3 by *Cr1KO* and *Cr1/2KO* mice. Immunoglobulin in response to DNP or TNP after immunization with the model immunogens TNP-LPS (TI-1), DNP-Ficoll (TI-2), TNP-KLH (10μg) or TNP-KLH (100μg) was measured at 0, 7, 14, and 21 days after primary immunization. Secondary immunizations were given to TNP-KLH immunized mice at 21 days and 28 day serum samples were also measured. Graphs show difference in absorbance of each mouse from the average WT absorbance at 490nm for each day. (TI-1 n=7–10; TI-2 n=9; TD (low) n=7; TD (high) n=10; 8–12 week old sex matched mice; all data represent a

composite of two independently performed immunizations; see Supplemental Figure 3) *B*, ELISA analysis of KLH specific IgM and IgG from TNP-KLH (100μg) immunized mice shown in panel *A* (n=10; 8–12 week old sex matched mice). *C*, ELISA analysis of SRBC specific IgM and IgG from mice immunized i.v. with 1×10^8 SRBC on days 0 and 21 (n=6; sex matched 8–10 week old mice). (One-way ANOVA performed for each day and Tukey's Multiple Comparison post test results shown for all time points found to be at least $p<0.05$ by ANOVA; *= WT compared to *Cr1KO*; #= WT compared to *Cr1/2KO*; */# = $p<0.05$; **/## = $p<0.01$; ***/###=$p<0.001$

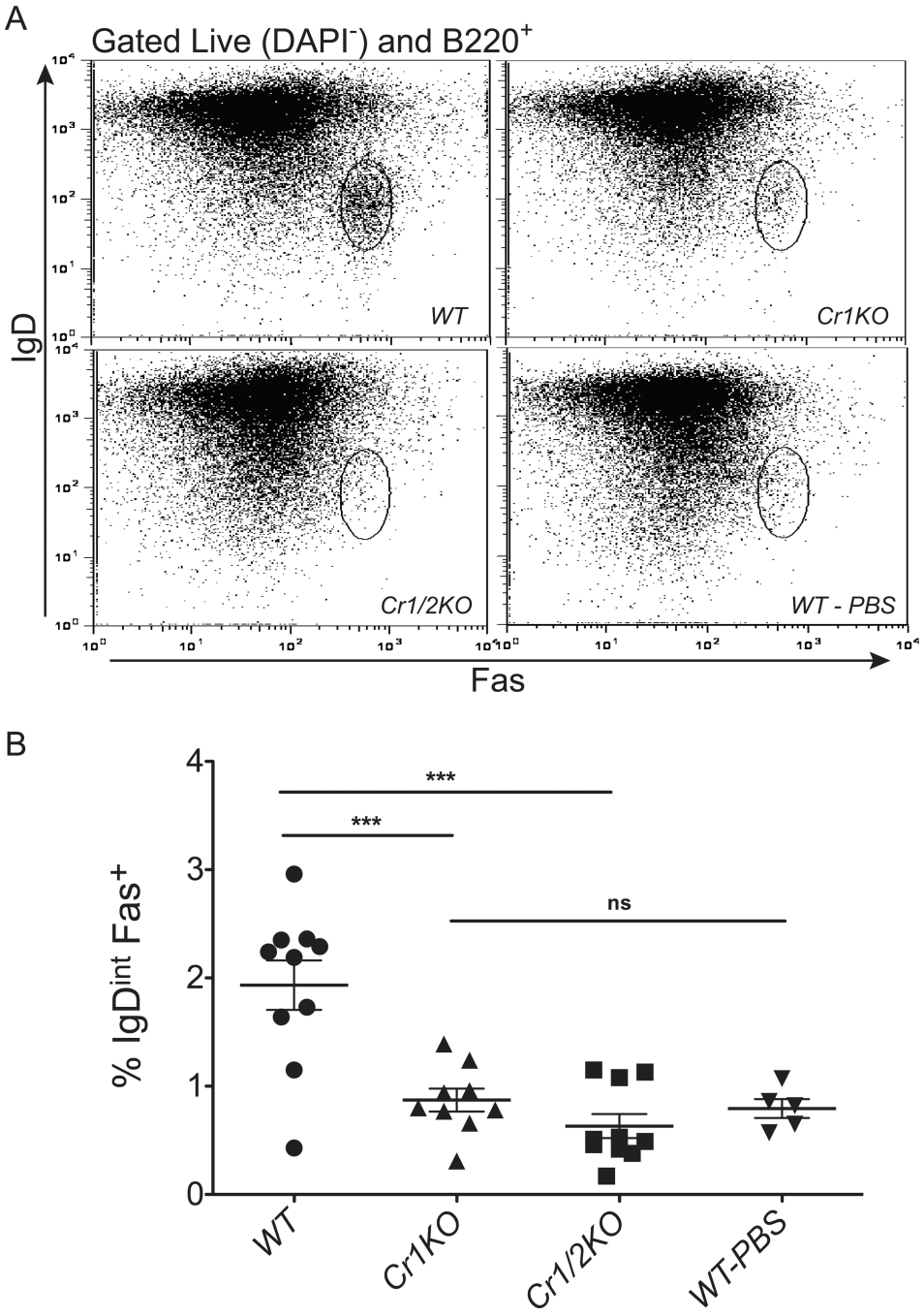

Figure 10.

FACS analysis of GC B cell frequency after SRBC immunization. WT, *Cr1KO*, and *Cr1/2KO* mice were immunized with 2×10^8 SRBC and isolated splenocytes were analyzed 7 days later. The IgD^{int} Fas^+ cells were gated from the total live $B220^+$ cells (*A*) and the average population percentage was graphed (*B*). (Error bars represent SEM; *=p<0.05, **=p<0.01 ***=p<0.001 by pairwise student's t-test; n=9–10 from three independent replicates of n=3–4; n=5 WT PBS treated; Sex matched 8–12 week old mice).

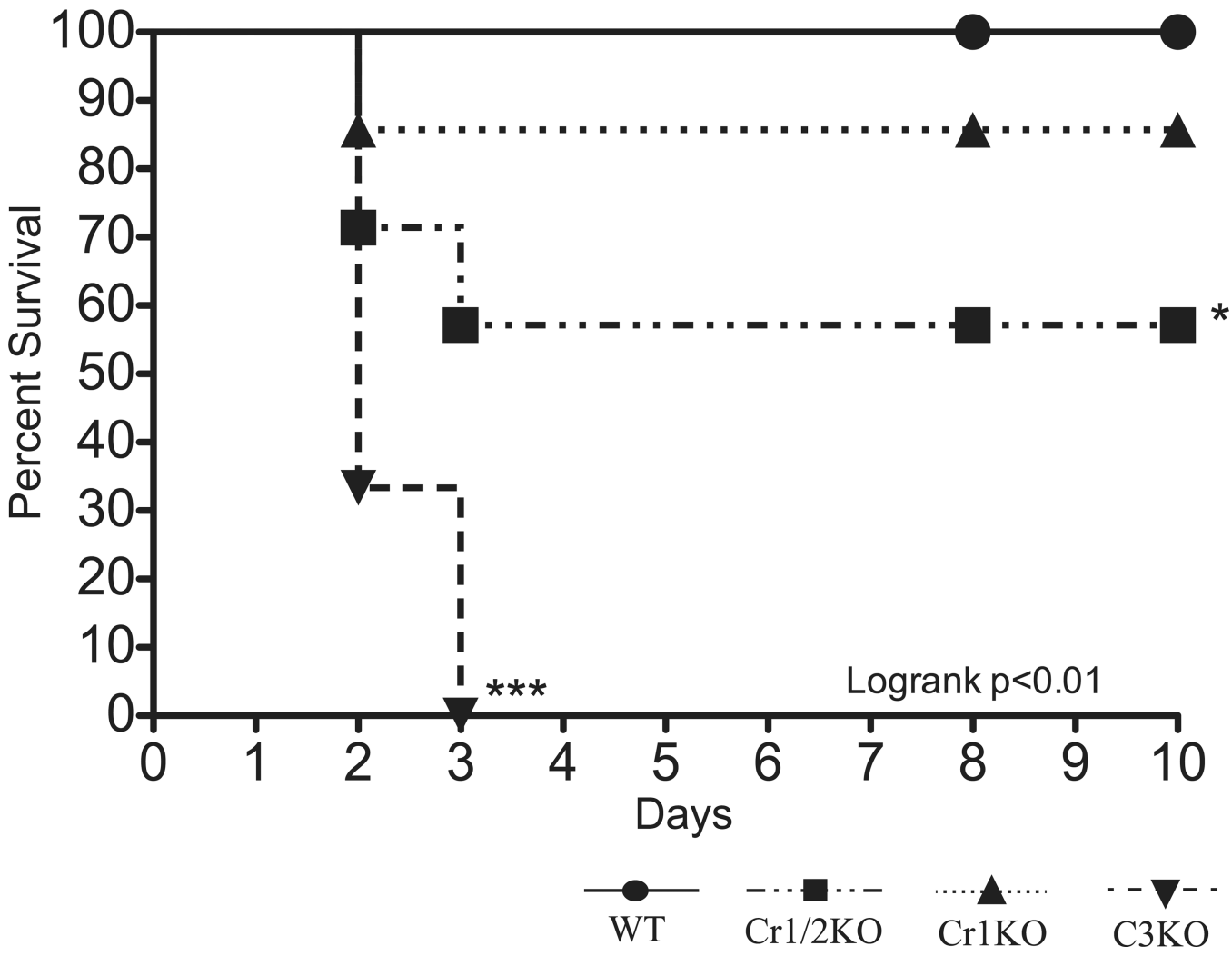

Figure 11.

Survival curve of *Cr1KO, Cr1/2KO, C3KO*, and WT mice after infection with *S. pneumoniae*. Mice were immunized with 1×10^5 heat-killed *S. pneumoniae* followed ten days later (0 days on graph) by infection with 1000 CFU of live *S. pneumoniae*. *Cr1KO* mice (dotted line) survive infection with *S. pneumoniae* at the same rate as WT. *Cr1/2KO* and *C3KO* mice survive significantly less frequently. (WT n=11, Cr1/2KO n=7, Cr1KO n=7, C3KO n=3;)